Seismic campaign for geothermal energy in the Netherlands (SCAN): an analysis of test line data quality

by Wouter Janssen

September 2019 - January 2020

Internship at Energie Beheer Nederland B.V.
Supervisor (EBN): Johannes Rehling
Supervisor (UU): Dr. Ivan Pires de Vasconcelos

Abstract

Seismic Campaign Geothermal Energy in The Netherlands (SCAN) was undertaken to fill the gap in subsurface data throughout the center and southern parts of the country. SCAN comprises of 2D seismic acquisition, re-processing of vintage data and, eventually, drilling exploration wells. Within SCAN, a test line was shot to determine optimal acquisition parameters. An investigation was performed into the quality of the test line seismic data, and its relation to acquisition parameter (e.g. shot depth, charge size) and external circumstances (e.g. wind, traffic). Seismic data shows a trend in shot quality that does not correlate to (a combination of) acquisition parameter(s) and is therefore likely controlled by the subsurface. Locally, however, data quality convincingly benefits from increasing charge size and shot depths. Noise mitigation can be performed through shooting with low wind speeds and keeping distance between source of noise and receiver. The south(eastern) part of the Flevopolder contains a source of high-frequency attenuation. Several culprits have been identified, the most likely being a thickened Eem-formation.

Contents

1 Introduction **3**

1.1 EBN & The energy transition . . . 3

1.2 Seismic campaign for geothermal energy in the Netherlands (SCAN) . . . 4

1.2.1 Geothermal plays . . . 4

1.2.2 Re-processing . . . 4

1.2.3 Acquisition . . . 4

1.3 Internship objectives . . . 9

2 Methods **10**

2.1 Noise amplitude analysis . . . 10

2.2 Signal amplitude analysis . . . 12

3 Results **14**

3.1 Ambient noise analysis in shot domain . . . 14

3.2 Signal analysis . . . 15

3.3 Signal-to-noise ratio (SNR) . . . 18

3.4 Frequency content . . . 19

3.5 Uphole time & uphole velocity . . . 21

3.6 Ambient noise analysis in receiver domain . . . 22

3.7 Noise analysis on stacked data . . . 27

4 Discussion **28**

4.1 Shot quality and geology . . . 28

4.1.1 The polder problem . . . 29

4.2 Noise mitigation . . . 31

5 Conclusion **32**

1 Introduction

1.1 EBN & The energy transition

In light of the energy transition ahead of us, the demand for sustainable and cleaner energy grows louder and more urgent rapidly. In an attempt to rid the Netherlands of fossil fuels and greenhouse emissions for 99% by 2050, geothermal energy might provide powerful means to reach this target. The accelerated termination of gas production from the Groningen gas field subsequently adds to a sense of urgency. The objective of geothermal exploration is to improve the sustainability of the heat supply for urban areas, industry and greenhouse farming regions. Here, geothermal energy would serve as a direct alternative to natural gas.

Energie Beheer Nederland B.V. (EBN) contributes to the energy transition through initiating projects such as, for instance, the decommissioning and re-using of oil and gas infrastructure in the North Sea, large-scale energy storage in hydrogen and Carbon Capture, Utilisation and Storage (CCUS) underneath the North Sea. In addition, the Dutch Ministry of Economic Affairs & Climate has awarded EBN a subsidy to perform geothermal exploration in collaboration with TNO (Netherlands Organisation of Applied Scientific Research).

The Netherlands is traditionally a gas-producing country and has locally explored its subsurface in detail. Naturally, these regions coincide with the location of oil and gas production which is concentrated mostly in the Northeastern part of the country. This leaves an hiatus in subsurface data availability in the Central and Southern parts of the country which consequentially prohibits the countrywide mapping of geothermal potential of the Dutch subsurface (Figure 1).

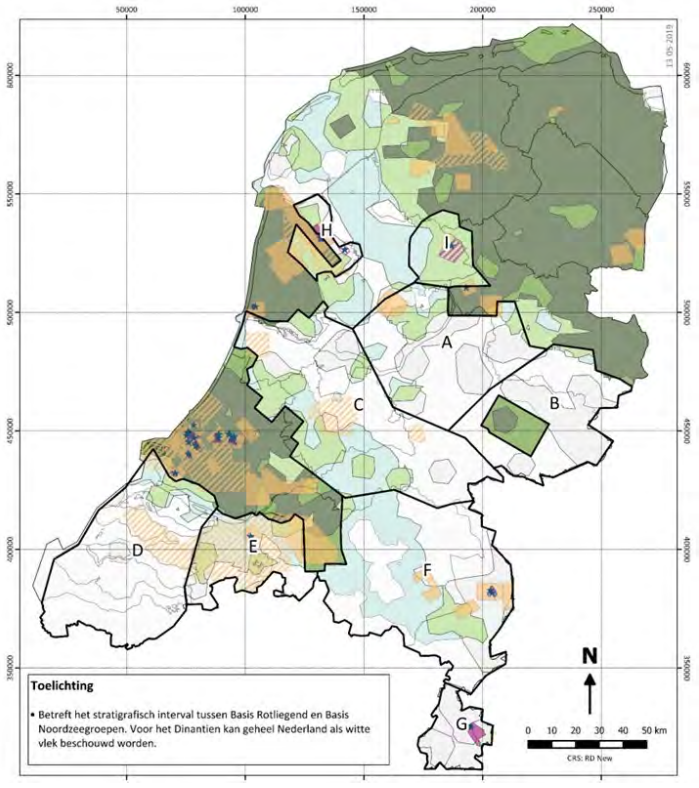

Figure 1: Present-day subsurface data availability for shallow geothermal targets Rotliegend and North Sea sandstones (UDG not included). The shades of green represent the amount of data constraining the depth, thickness and quality of the reservoirs. Green represents well constrained, white means not constrained. *Source: TNO & EBN*

1.2 Seismic campaign for geothermal energy in the Netherlands (SCAN)

1.2.1 Geothermal plays

The SCAN-project is the geothermal exploration program undertaken by EBN and TNO to produce subsurface models with increased resolution and decreased uncertainties regarding the the presence, thickness and position of geothermal reservoirs in localities of limited data availability. The SCAN-project was initiated in 2017 and comprises of the re-processing of vintage 2D seismic data, acquisition of 2D seismic data and the drilling of geothermal investigation wells. The aim is an improved imaging of the four potential geothermal plays that have been identified in the Dutch subsurface; these being:

1. **Cenozoic sandstones**
   Present in most areas at a depth between 500m and 1500m.

2. **Triassic sandstones**
   Present in the south of the Netherlands at a depth between 1000 and 3500m.

3. **Permian Rotliegend sandstones**
   Present in the center of the Netherlands at a depth between 1000m and 3500m.

4. **Dinantian carbonates:**
   The Ultra Deep Geothermal play (UDG), as identified by Boxem et al. (2016), which is possibly present in the center and northern parts of the Netherlands at a depth of $4 - 6.5$km. The Lower Carboniferous Dinantian carbonates are expected to contain high temperatures of $> 120\text{C}^{\circ}$. However, reservoir presence and structure remain ill-constrained. Currently, multiple studies are being performed on, for instance, the productivity, injectivity, risk assessment, geotherm and porosity of the Dinantian carbonates (e.g. Bruijnen (2019); Carlson (2019); Middelburg and Drenth (2019)). At present, not a single ultra deep geothermal project is operational in the Netherlands.

1.2.2 Re-processing

During an inventory study within SCAN, over 700 vintage 2D seismic lines from 1970 onwards were identified for potential re-processing (Figure 2). Using state-of-the-art processing techniques, re-processing of 24 Mobil lines (314 km, 1984-1988, dynamite & vibroseis) and 2 NAM-DEEP lines (800 km, 1982 & 1984, dynamite) was performed over 2018 and 2019. Attempts were made at improving the seismic resolution and thus improving the imaging of faults and the presence of thickness of clastic reservoirs (including the UDG-target).
Re-processing results shows improvements in the signal-to-noise ratio and overall event continuity (Figures 4 and 5). Deep imaging (below $\sim 2 - 2.5$ TWT) does not always improve significantly. At the time of writing, new lines were being chosen for further re-processing.

1.2.3 Acquisition

To tackle the data gap issue as illustrated in Figure 1, the foremost intention is to acquire new high-quality subsurface data through seismic 2D surveys. The total length of seismic 2D acquisition within SCAN is estimated to be around 2000 km. At the time of writing, several lines were shot in area C (Figure 1), through the provinces Flevoland and Gelderland.

In early 2019, EBN shot a 2D seismic test line to evaluate how 2D seismic data acquisition using state-of-the-art wireless equipment compares to 2D vintage data from the 1980s. The chosen line was already part of the SCAN program and will therefore also be used for the imaging of geothermal targets. This particular line has been designated as the test line because it crosses both polder and 'mainland' regions and is therefore likely to have variability in subsurface characteristics. The test line is meant to produce a data set to establish the most favorable acquisition parameters for the future lines of the SCAN project - which is a trade-off between data quality, acquisition costs and duration of acquisition. The test line was a long offset line with a dense shot and receiver spacing; this configuration allowed for depopulation tests in the processing of the seismic data. The test line has a partial overlap with a part of the NAM DEEP lines which, in turn, serve as a benchmark in terms of resolution and subsurface structure (Figures 6 and 7). Several shots (20 shots on each end with a shot spacing of 200 m) were shot outside the receiver array, to test the contribution of ultra-long offsets.

Table 1 shows the acquisition parameters for the test line. The test line ran roughly from Maartensdijk to Almere Hout (line C in Figure 2) and crossed 9 municipalities. The footprint was kept to a minimum by using wireless geophones and the acquisition went without safety incidents. The size of the detonated dynamite charges is regulated and dependent on the proximity to, for example, gas lines, sewage pipes, dikes, buildings etc. The drilled holes were plugged using bentonite, which swells significantly when hydrated, in order to seal the affected layer(s) and prevent groundwater ingress. Shot depths were locally limited (the shot depth in Flevoland was restricted due to regulation regarding groundwater extraction) although the aim was maximum of 18 m. The survey itself was outsourced to Rossingh Drilling B.V. (shot hole drilling & shooting) and to Geofizyka Torún S.A. (receiver spread & data processing).

Acquisition	**Design outcome**
Line length	37 km (29 km receiver spread)
Dates	21-02-2019 until 22-03-2019
Source	Explosive
Charge size	220-1320 g
Max. shot depth	18 m
Receiver spacing	5 m
Shot spacing	20 m
Receiver type	5 Hz wireless geophone
Number of shots	1355
Number of receivers	5629
Number of traces	∼7.5 million

Table 1: The test-line acquisition parameters.

Results of the processed test line data generally shows a substantially higher resolution compared to the re-processed NAM-DEEP line (Figures 6 and 7). The conclusion that can be drawn from the depopulation tests is that, as expected, a higher density of shots and receivers yields an improved signal-to-noise ratio and crisper events. However, the differences in imaging are subtle. Unfortunately, the imaging beneath 3 seconds TWT (where the Dinantian reflector is expected) did not improve much. From the depopulation results it was concluded that further lines within SCAN will be shot with a shot spacing of 60m and a receiver spacing of 5m. Further increasing shot or receiver spacing would impair the imaging of faults and steep reflectors. Also, future SCAN seismic data will be acquired without shots outside the receiver spread. Forming a receiver array, where you sum with neighbouring traces, turned out not to be fruitful.

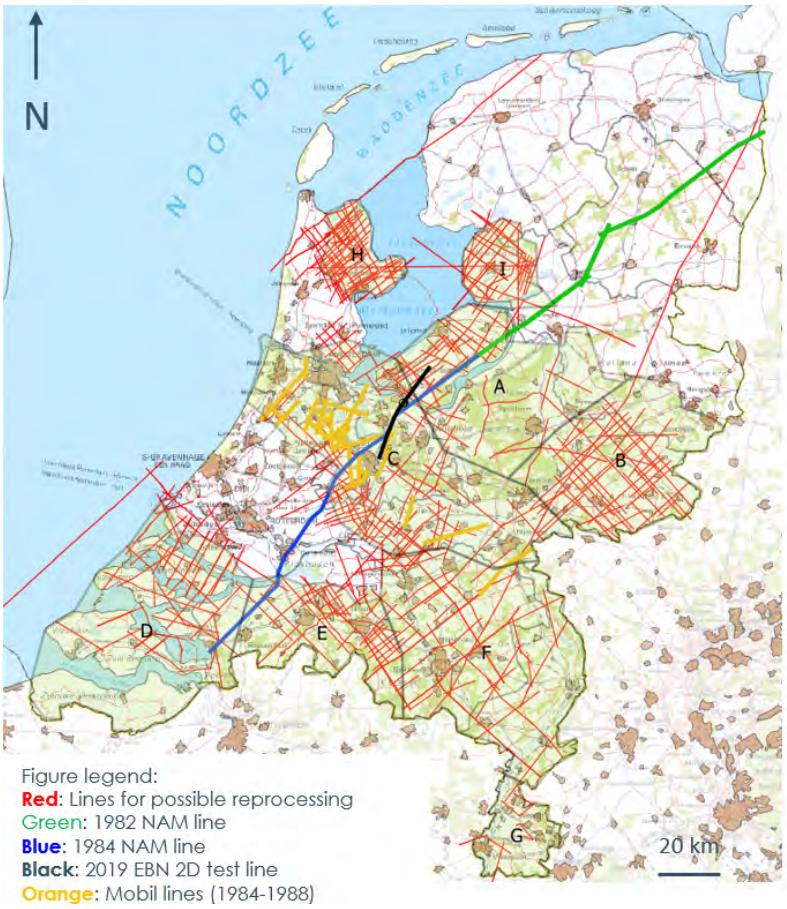

Figure 2: The result of an inventory study into 2D vintage seismic lines in the Netherlands which are candidates for re-processing (red lines). The combined green and blue line represent the NAM-DEEP line, the orange lines represent the reprocessed Mobil lines and the black line represents SCANs test line - which has partial overlap with the NAM-DEEP line. *Source: EBN*

Figure 3: The planning for the SCAN 2D seismic acquisition. A solid line represents a seismic line that is either planned, currently being shot or finalized. A dashed line represents an optional survey extension. *Source: http://www.scanaardwarmte.nl*

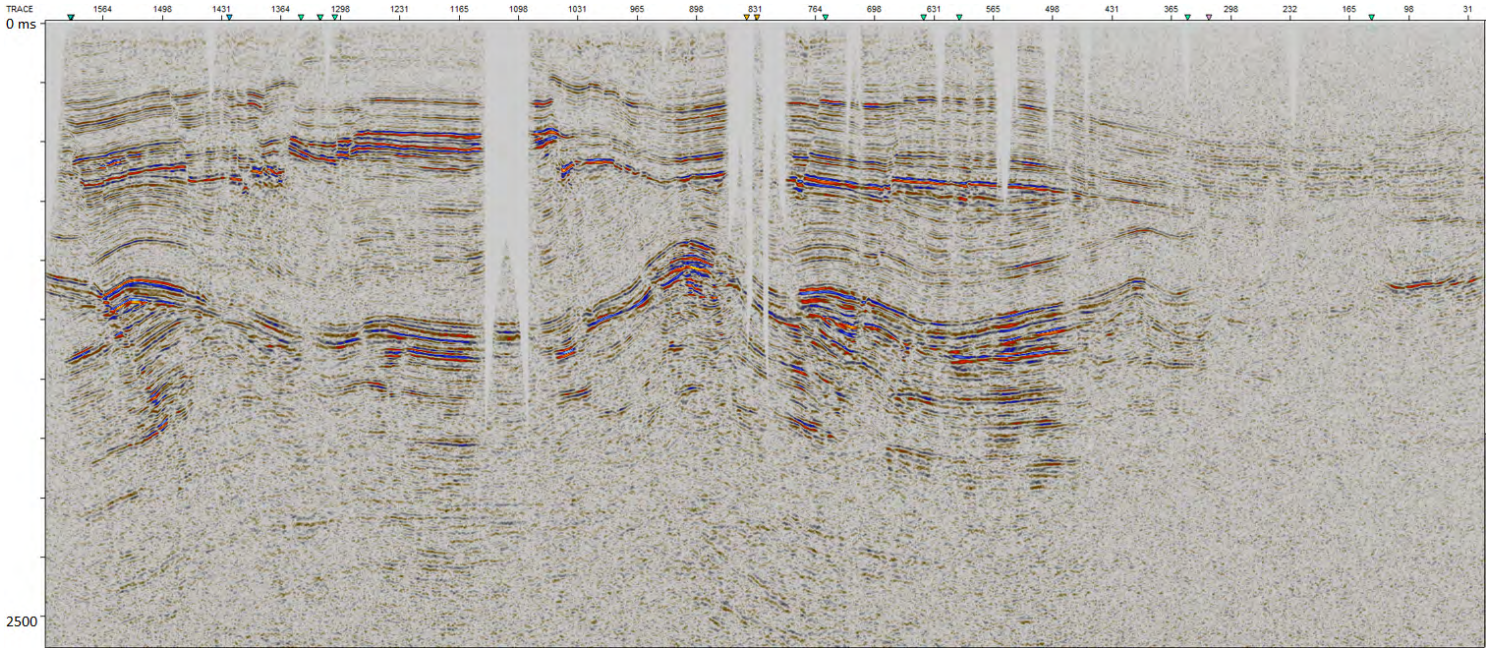

Figure 4: Vintage 2D seismic line MZ85-57 (1985) from Mobil. *Source: EBN*

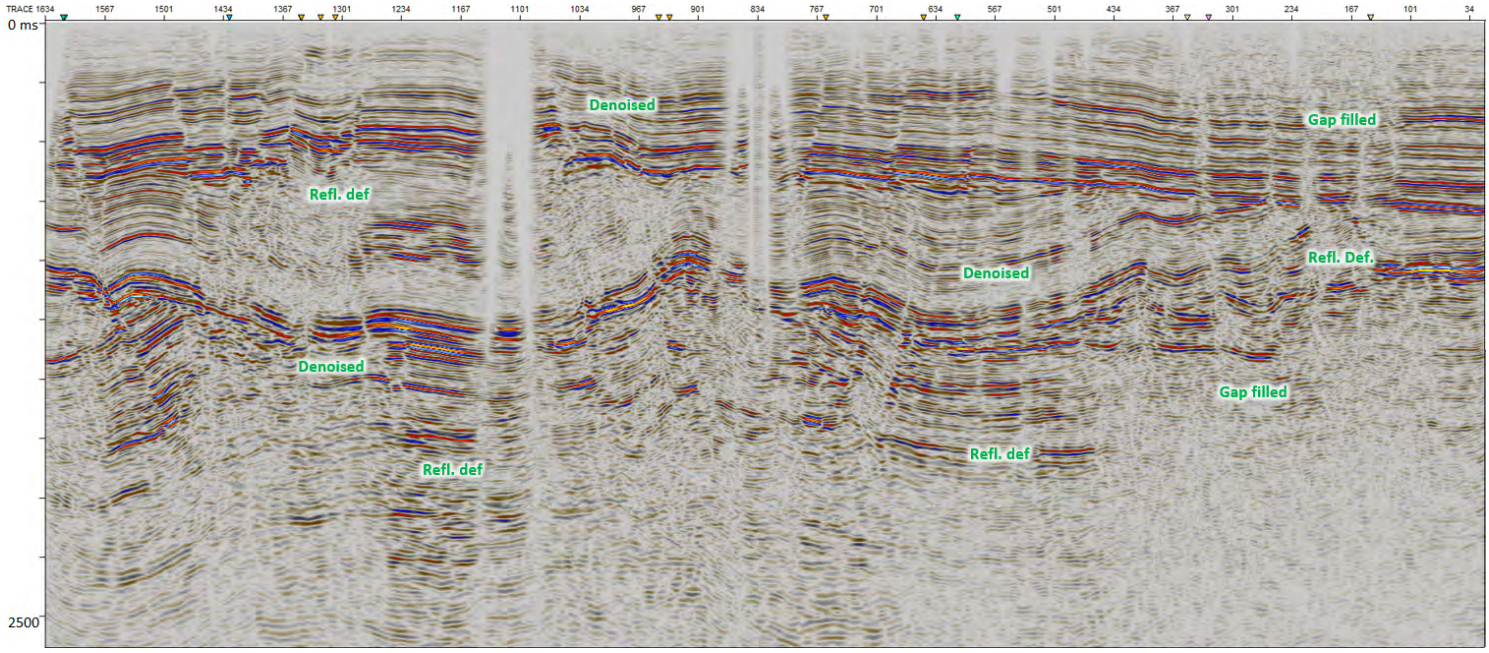

Figure 5: Re-processed 2D seismic line MZ85-57 (PreSTM). Compared to figure 4, events show better continuity and are generally more crisp. Deep imaging did not significantly improve and the top of the Dinantian is not visible. *Source: EBN*

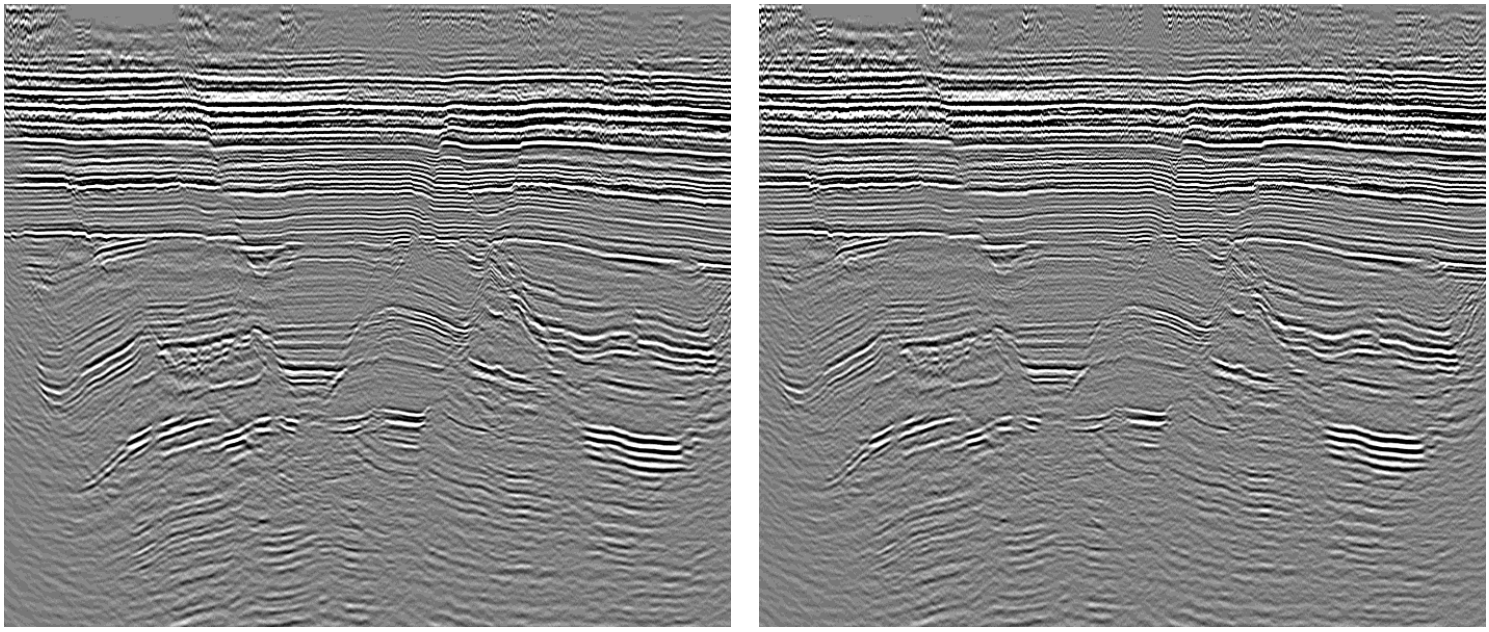

Figure 6: Shot depopulation: The preliminary test line PreSTM images with a shot spacing of 20m (left) and 60m (right). Time window: approx. 0-2100ms.

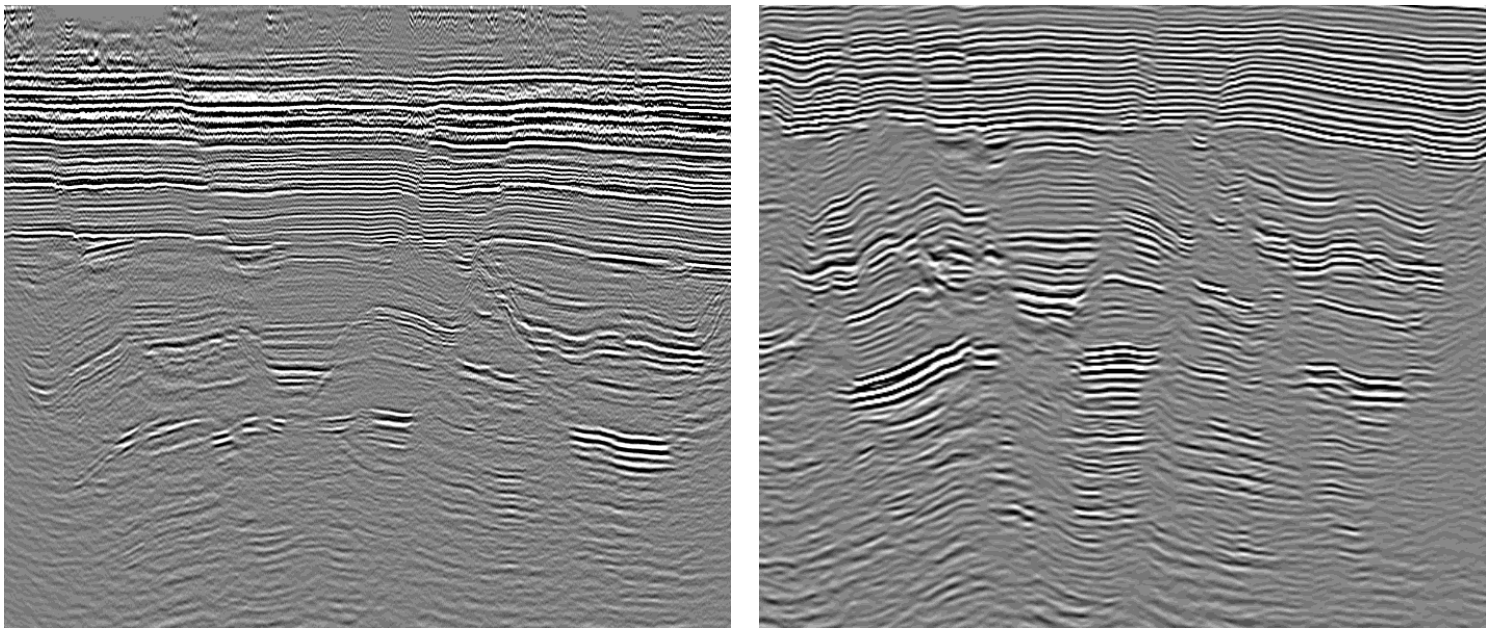

Figure 7: The preliminary test line PreSTM with a shot spacing of 100m (left) and the PreSTM re-processed NAM-DEEP line. Time window: approx. 0-2100ms.

1.3 Internship objectives

This project requires a very thorough understanding of seismic shot quality, not only the final migrated seismic images. Due to the test line having such a high density of shots and receivers, it is an ideal data set to help answer the research questions as stated below. This internship is an investigation into the shot quality of SCANs test line and any learning from the acquisition, the detailed field data analysis and processing of the test line will feed back into the SCAN seismic acquisition programme, that is being executed at the time of writing.

Research questions:

1. What is the relationship between shot data quality* and weather (particularly wind noise)?
2. What is the relationship between shot data quality* and traffic noises?
3. What is the relationship between shot data quality* and time of shooting, e.g. morning, mid-day, afternoon or evening?
4. What is the relationship between shot data quality* and shot depth?
5. What is the relationship between shot data quality* and charge size?
6. What is the relationship between shot data quality* and near surface geology (based on available data from DINOloket)?
7. What is the relationship between shot data quality* and measured uphole times?
8. What is the relationship between the measured uphole time and the near surface geology?
9. Can we make recommendations on shot design based on near surface geology?
10. What is the relationship between ground roll variation (e.g. dominant frequency, ground roll velocity) and near surface geology?

*Shot quality evaluated based on signal amplitude, amplitude spectrum, (time and offset window-based noise analysis and ground roll (analysed in time and F-k domain).

2 Methods

Firstly, in order to answer the research questions, a definition of shot quality had to be established. For seismic data, this is done through the signal-to-noise ratio (SNR). In this case shot data is investigated, therefore the amplitudes of the signal and noise have been quantified in the shot domain. All seismic data analysis and visualization has been performed in GLOBE Claritas^{TM}.

2.1 Noise amplitude analysis

RMS noise amplitudes per individual trace per shot gather have been quantified in GLOBE Claritas ^{TM}, which contains options to prescribe time and offset windows. To obtain a quantification of ambient noise, RMS amplitudes were summed and divided by the number of non-zero traces, in either shot or receiver domain. The ambient noise amplitudes were performed in the last second of each shot gather, which is 19-20s, using all traces and under the assumption no more shot energy is present in this time window. This was tested against ambient noise amplitudes in the first second of all shot records, yet in an offset range which does not contain any shot energy (Figure 8). The results from these noise analyses showed consistent behaviour (Figure 9). To utilize all traces, the ambient noise amplitudes from the last second of the shot records have been used for further analyses (see Results).

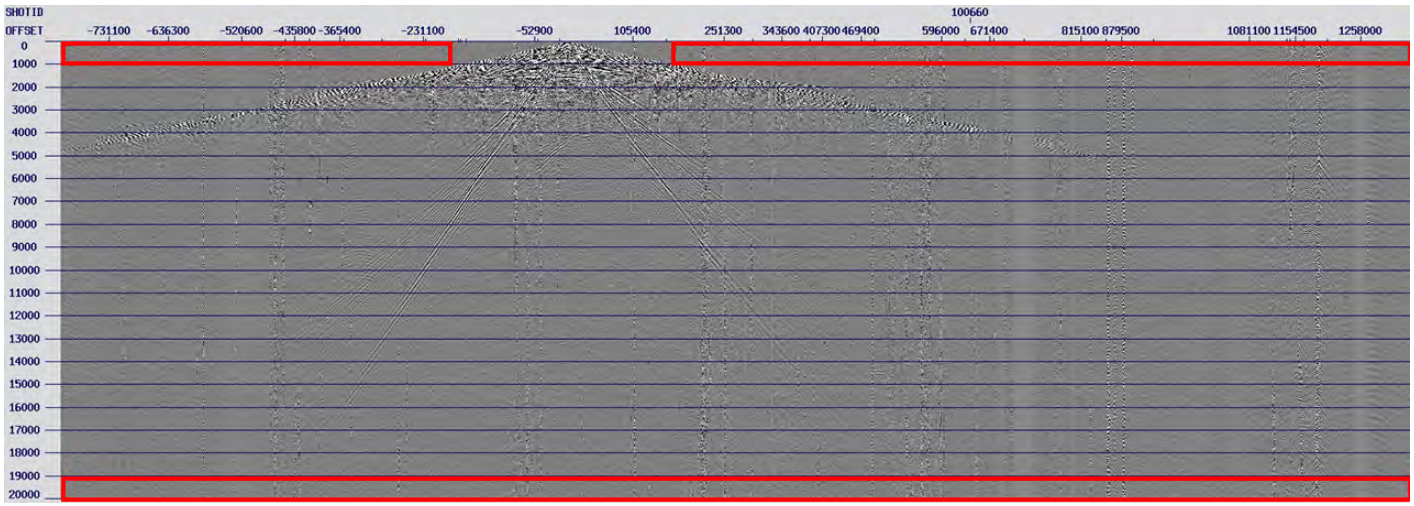

Figure 8: Two ambient noise measurements visualized on a shot: a measurement in the last second (19-20s) containing all traces (bottom) and a measurement in the first second (0-1s) containing traces in an offset range that does not contain shot energy (top). Vertical axis states time in ms.

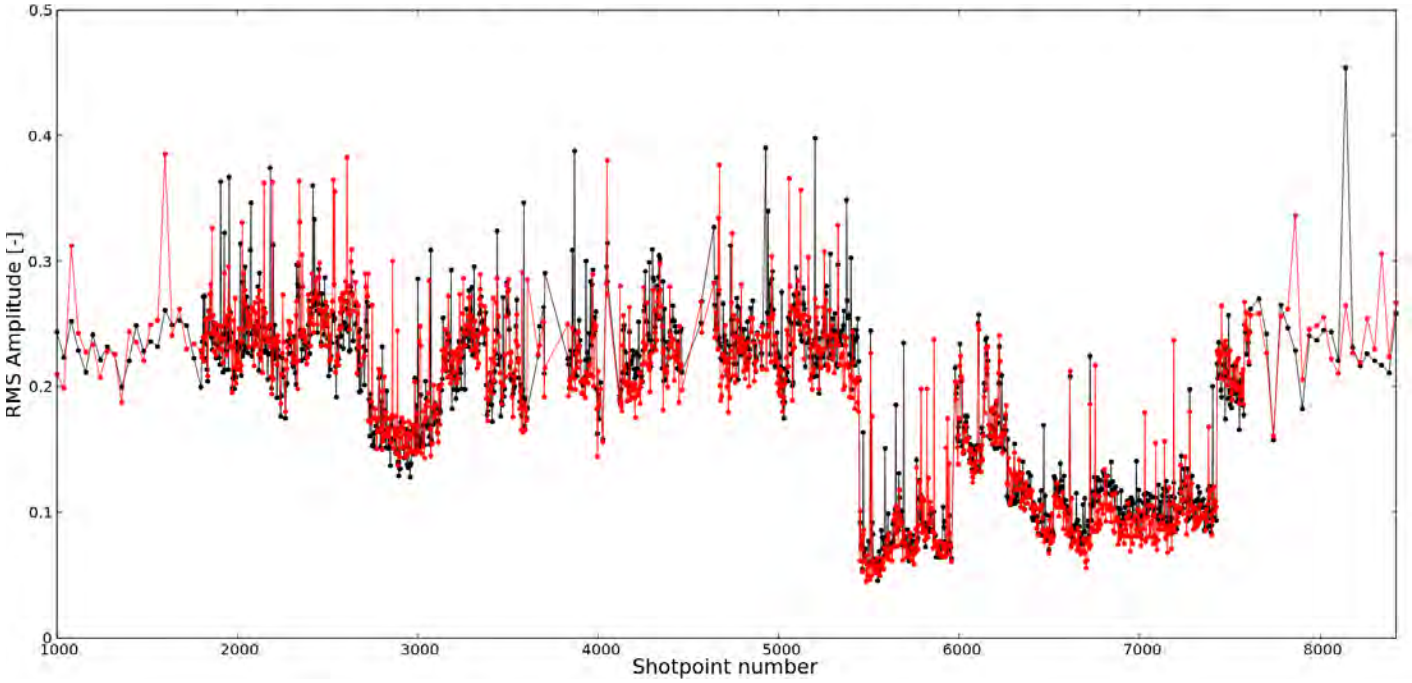

Figure 9: Noise amplitudes per shot gather measured over the first second (red, excluding shot energy) and the last second (black). Left=SW, right=NE.

2.2 Signal amplitude analysis

A quantification of the signal amplitude per shot gather was obtained through the averaging of RMS amplitudes of the traces in the first second, in an offset range without any ground roll (Figure 10). Attempts have been made to filter the ground roll using high-pass filters, frequency-wavenumber filters and combinations thereof (Figure 11) in order to broaden the offset range. However, this was hindered by the low frequency signal content in the northernmost part of the test line which left residual high-amplitude ground roll energy in the RMS amplitude analyses (see Results). Here, due the overlapping frequency content of ground roll and signal, the ground roll cannot be wholly removed using a frequency-dependent filter. It can be removed with a Tau-P filter, however, this was not prioritized in this research. The signal amplitude was measured in offset range [-175000:-35000] cm and [35000:175000] cm (Figure 10). Shots fired outside the receiver spread were not taken into account in the data quality analysis, for no signal amplitude measurement could be performed. All measurements were performed on raw data.

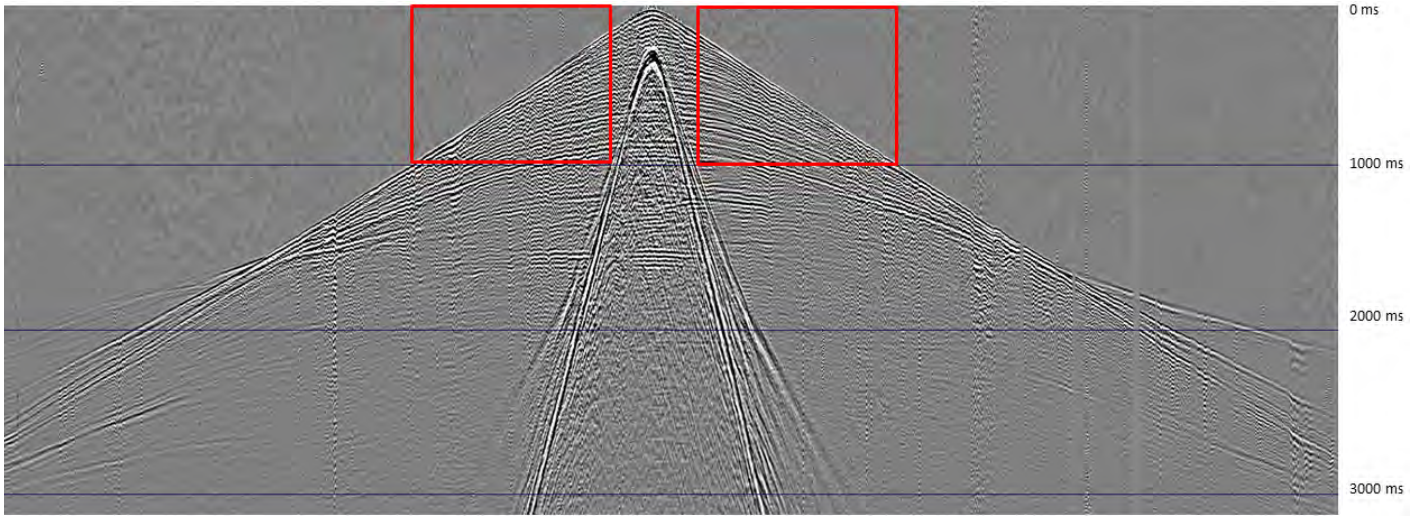

Figure 10: A visualization of the time and offset range in which the RMS signal amplitudes were measured. The measurements do not contain ground roll amplitudes.

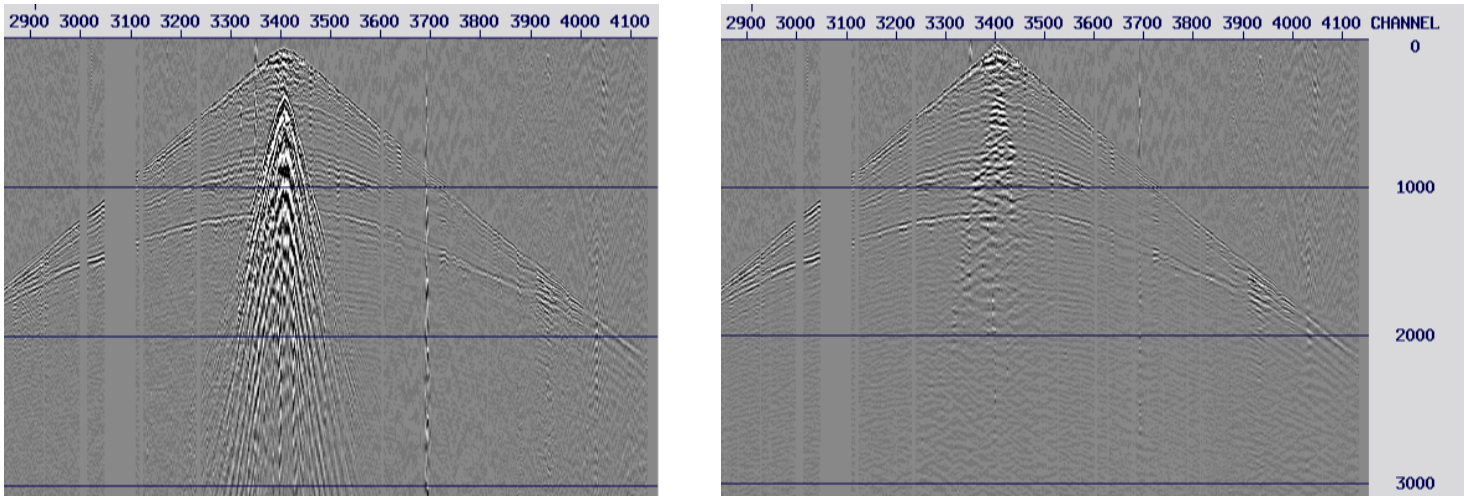

Figure 11: A shot gather located in the polder: raw (left) and after a high-pass filter (taper 7-10Hz) and a subsequent f-k filter (right). Residual ground roll amplitudes remain which can't be removed using a frequency-dependent filter without affecting the signal. Vertical axis states time in ms and horizontal axis states trace numbers.

Quantification of signal and noise permits the calculation of the SNR by a simple division. The definitions of the signal and noise amplitudes per shot gather, as well as the SNR, allow shot quality to be correlated to metadata related to acquisition and external circumstances. Acquisition parameters are shot depth, charge size, location and crew ID. External circumstances are, for instance, time of shooting, windspeed and proximity to sources of noise. Quantifying signal amplitudes also allows for the identification of poor quality shots along the line. Measurable variables such as uphole times (and uphole velocity), dominant frequency of both signal and ground roll are correlated to the local (near surface) geology.

Geological cross-sections were extracted from 3D geological model DGM and REGIS II, which are interpolations of well-data (available at DINOloket), and visualized in SubsurfaceViewer. These geological models consist of a 3D framework in which the top, base and thickness of each unit is defined. Although it is a mere interpolation of basal surfaces of the units, the interpolation procedure is adapted to take into account geological formation-specific characteristics and depositional history, as well as major faults present in the Netherlands (Gunnink et al. (2013)).

The effect of the groundwater table on the seismic data was investigated, however, a lack of data quantity and quality prohibited a meaningful analysis. Groundwater data, available at DINOloket, is often outdated and suffers strongly from seasonal and annual variability.

Map-view figures were constructed in QGIS. Also measurements of distance were taken from QGIS.

3 Results

3.1 Ambient noise analysis in shot domain

Analysis of ambient noise amplitudes (19-20s; all traces) in the shot domain can be correlated to external circumstances such as the time of shooting (Figure 12) and wind speeds (Figures 13 and 14). Hour-averaged wind speed data originates from KNMI (The Royal Netherlands Meteorological Institute).

Noise amplitudes per shot gather can be significantly reduced by either shooting before 9am, after 6pm or with low wind speeds. It must be noted, however, these two variables are often mutually correlated, the afternoon generally being the windiest time of day.

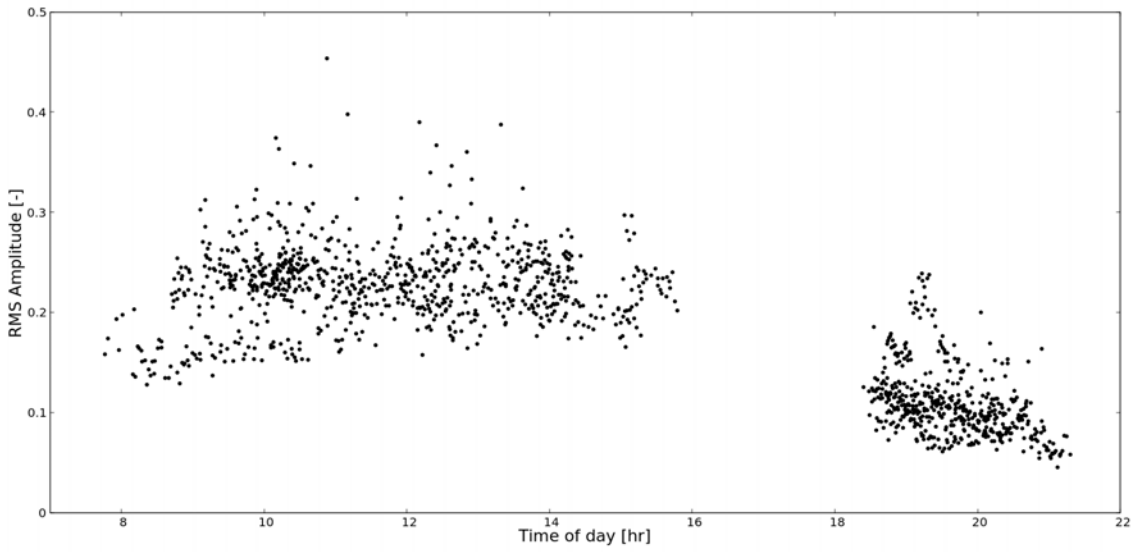

Figure 12: The RMS noise amplitudes per shot gather versus the time of time of shooting.

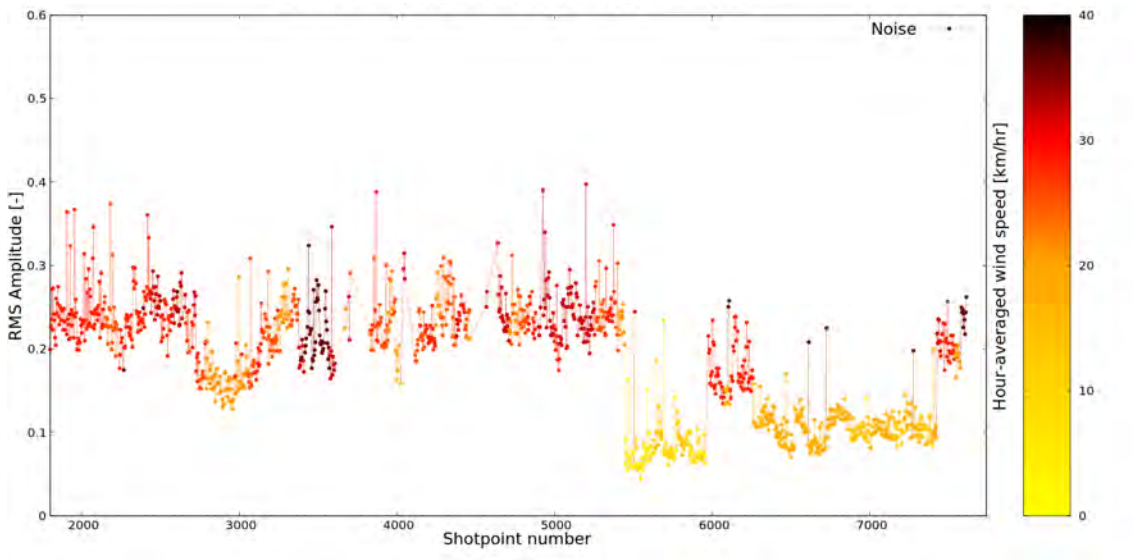

Figure 13: The RMS noise amplitudes per shot gather versus shotpoint number (left=SW, right=NE). The colour coding represent the hour-averaged wind speeds from the KNMI.

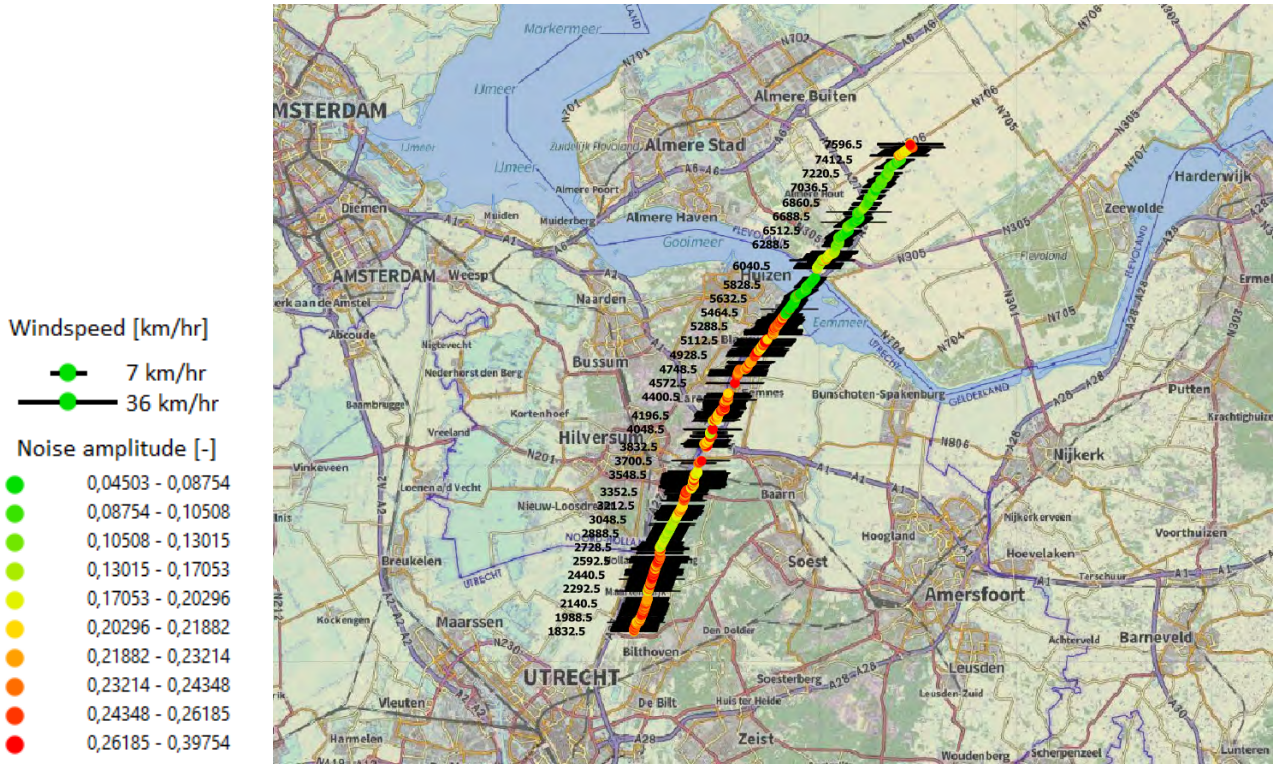

Figure 14: Map-view (1:165000) of noise amplitudes per shot gather. The colour coding represents noise amplitudes and the line-marking represents the wind speed at the time of shooting (between 7 and 36 km/hr).

3.2 Signal analysis

Signal amplitudes show significant variation throughout the test line. Quantification of the signal amplitudes per shot gather allowed for the identification of 'weak shots', which are shots whose energy content are significantly lower than local average (Figure 14). Over the SCAN test line, 72 of such shots were identified (5.3% of the total amount of shots). Shots acquired at shotpoint numbers $\geq$ 5976.5 consistently yield low amplitudes, although they have often been acquired using 880-1000gr dynamite at a depth of $\geq$ 10m (Figure 15). This coincides with the province of Flevoland which is an empoldered region. Here, a notably different near-surface geology is expected due to these areas having been seafloor before 1955-1963. The southern part of the test line, roughly between shotpoint numbers 2700-3500, yields the highest signal amplitude along the line. This area of high signal amplitudes is in the vicinity of stowed glacial deposits. Also, these shots have been acquired in wooded areas, where the ground is possibly more consolidated compared to cultivated pastures. The dominant trend and largest variations in signal amplitudes can not be correlated to (a combination of) acquisition parameters(s). Locally, however, it is clear that maximizing shot depths and charge sizes is beneficial to signal amplitudes. As a result of regulations on the permitted peak-particle-velocity at the surface during seismic acquisition, shallow shots often coincide with lower charge sizes.

Figure 15 displays geological model REGIS II, which is the highest resolution model comprising subsurface data along the entire test line. It must be noted that geological models are mere interpolations of well data and accompanied uncertainties should be taken into consideration (see Discussion). The relevant geological models available at DINOloket (REGIS II, GeoTOP and DGM) agree on the presence of these stowed glacial deposits, however, GeoTOP contains a different relief of this formation compared DGM and REGIS II.

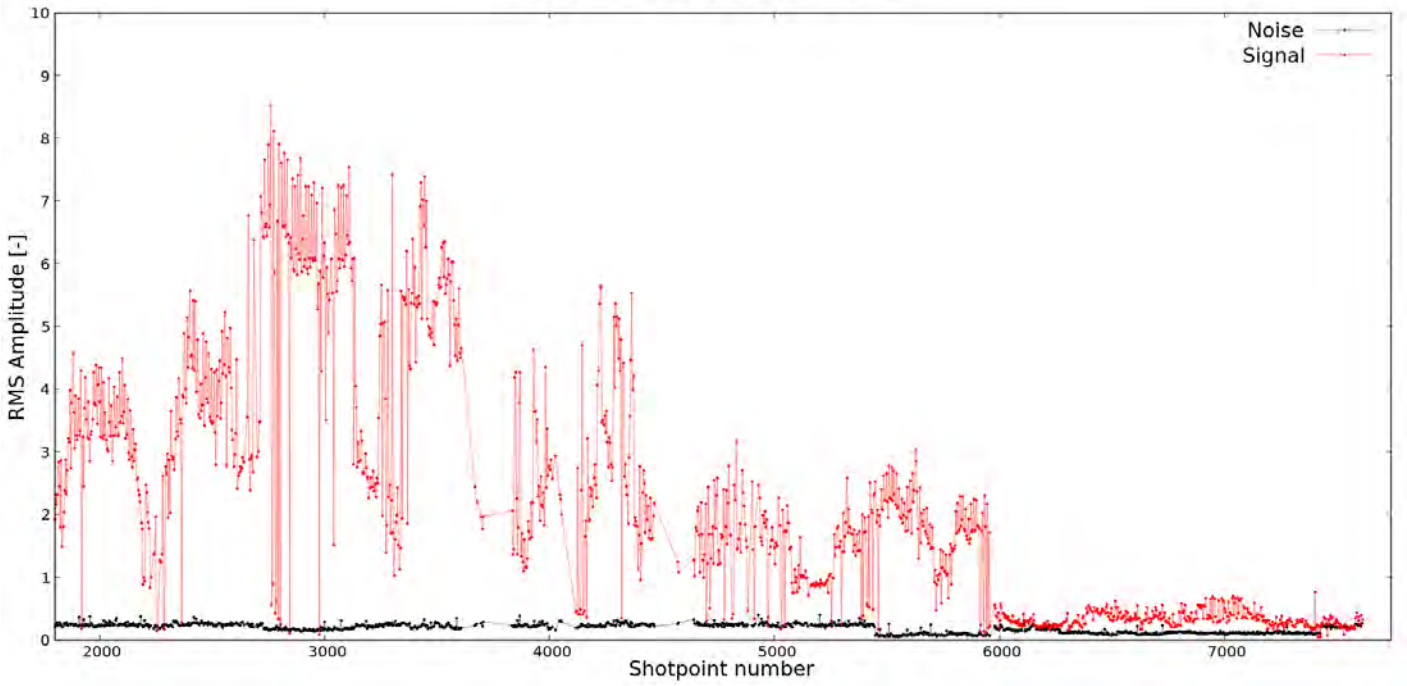

Figure 14: Signal amplitudes (red) and noise amplitudes (black) per shot gather versus shotpoint number (left=SW, right=NE).

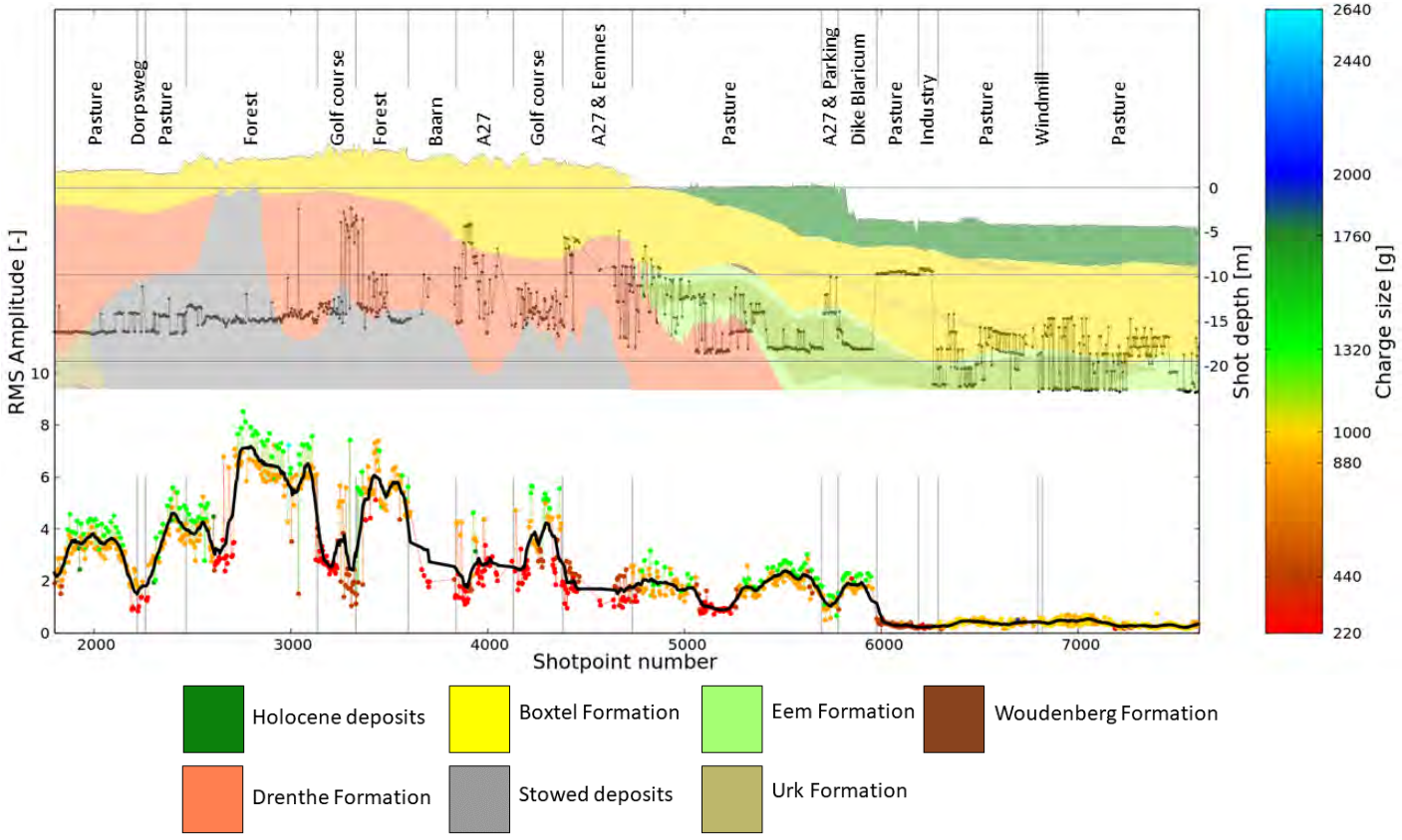

Figure 15: The signal amplitudes per shot gather accompanied by a 15-point moving average (black). Colour coding represents the charge size (see colourbar). Above it, geological model REGIS II (available at DINOloket, legend below figure) and the elevation-corrected shot depth and thus, theoretically the geological formation the shots were fired in. At the top, surface characteristics along the line. This figure excludes the shots flagged as 'weak'. Left=SW, right=NE.

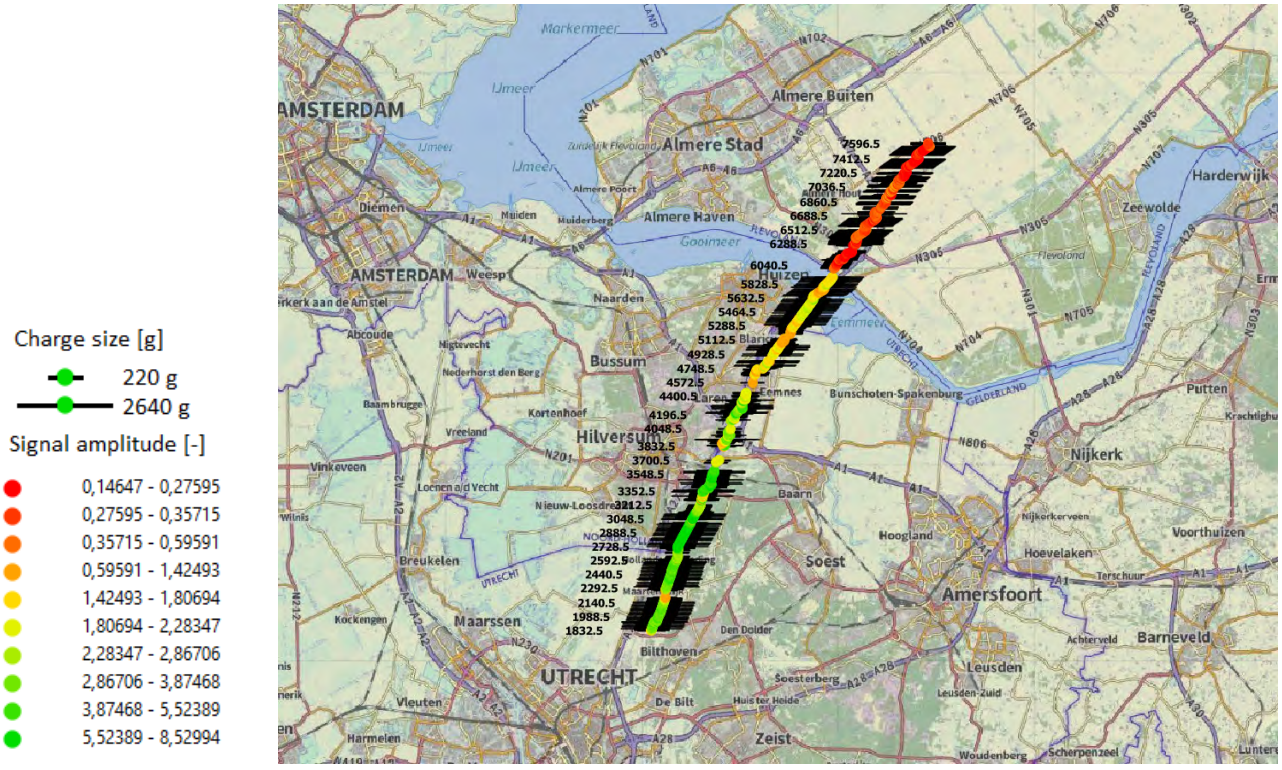

Figure 16: Map-view (1:165000) of signal amplitudes per shot gather. The colour coding represents signal amplitudes and the line-marking represents the charge size (between 220 and 2640g).

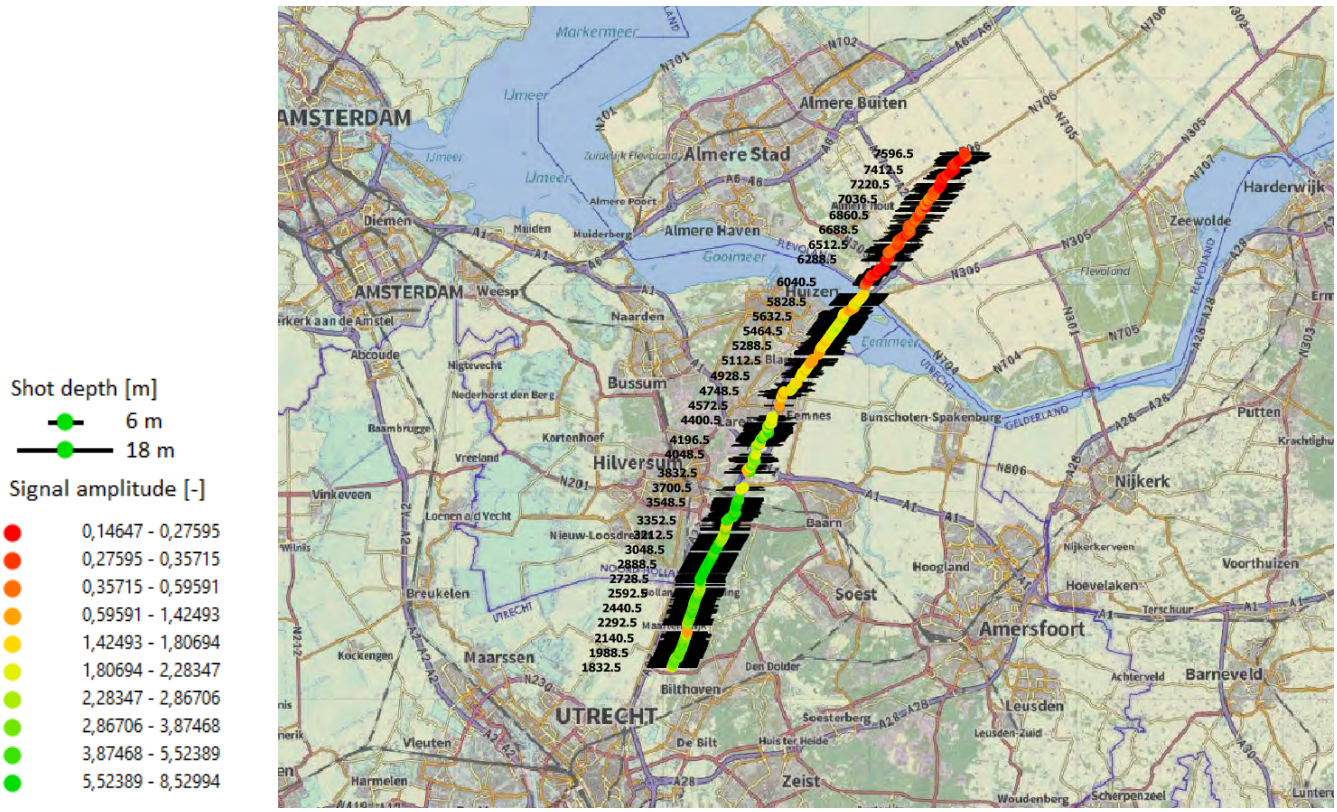

Figure 17: Map-view (1:165000) of signal amplitudes per shot gather. The colour coding represents signal amplitudes and the line-marking represents the shot depth (between 6 and 18m).

3.3 Signal-to-noise ratio (SNR)

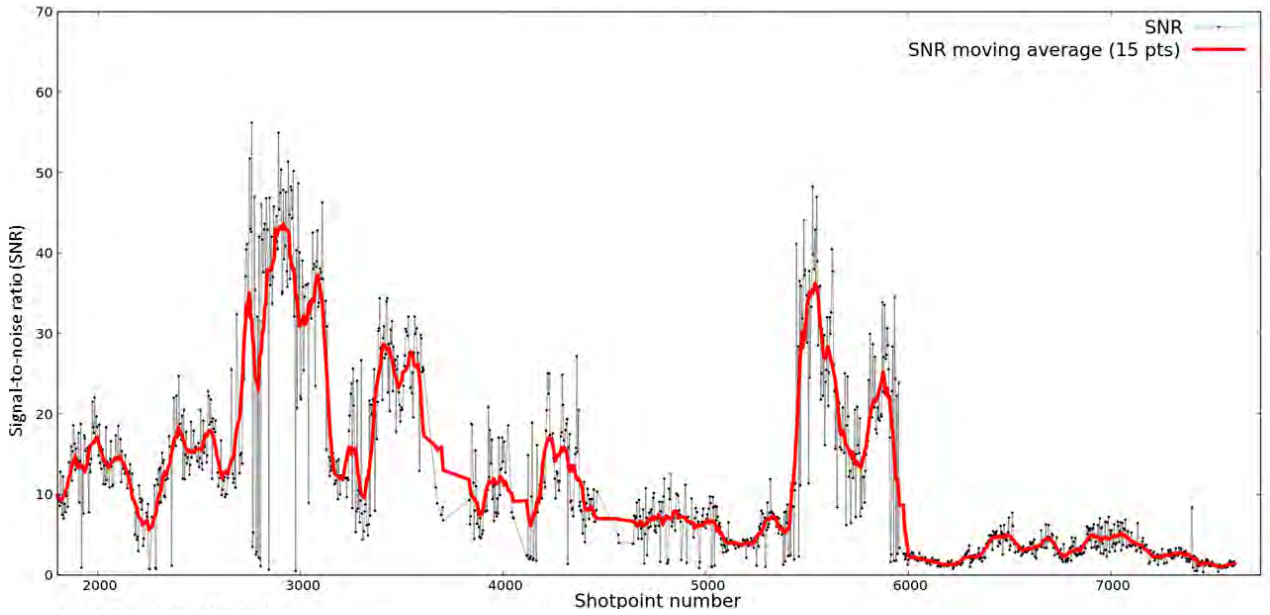

Figure 18: The SNR for the test line, including shots flagged 'weak' (left=SW, right=NE).

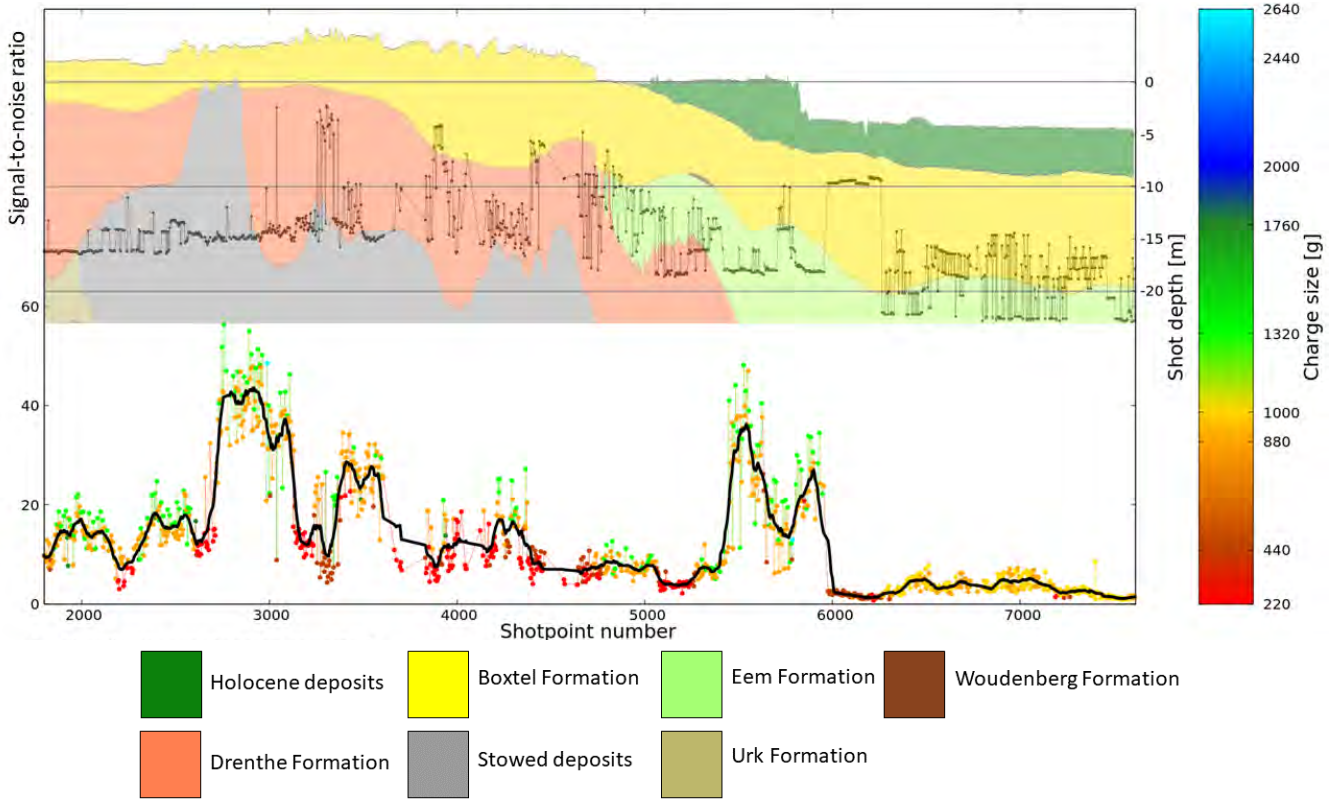

Figure 19: The SNR per shot gather accompanied by a 15-point moving average (black). Colour coding represents the charge size (see colourbar). Above it, geological model DGM (available at DINOloket, for legend see Figure 15) and the elevation-corrected shot depth and thus, theoretically the geological formation the shots were fired in. This figure excludes the shots flagged as 'weak' (left=SW, right=NE).

The SNR, used as a quality measure per shot gather, is established using the aforementioned definitions of signal and noise amplitudes. The SNR also shows significant variation in magnitude along the test line (Figure 18). Consistent with signal amplitudes, the SNR is low in empoldered regions and high in the wooded areas around Hilversum (Figures 19 and 20). The SNR is consistent with the signal amplitudes, however, shots acquired at low noise levels (low wind speeds) will peak in the SNR analysis. For instance, in contrast to the signal amplitudes (Figure 15), the SNR peaks approximately around shotpoint numbers 5500-6000, which is due to low wind speeds at the time of shooting (Figure 13).

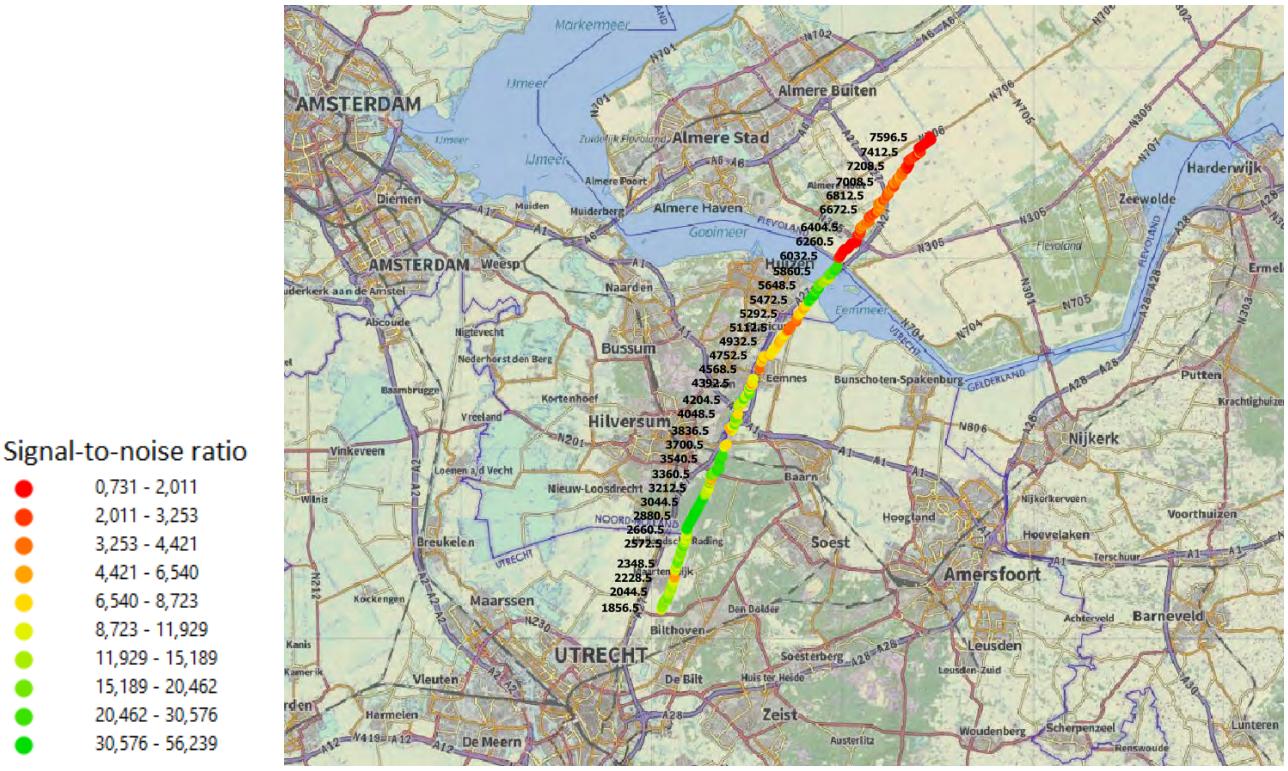

Figure 20: Map-view (1:165000) of the SNR per shot gather.

3.4 Frequency content

The dominant frequencies for every third shot gather has been hand-picked from the shot record (Figure 21). The dominant ground roll frequency is consistent throughout the line, averaging 6-8 Hz. In the southern and middle part of the test line, signal frequencies range around approximately 20-50 Hz. In the northern part of the line, however, the dominant signal frequencies abruptly converges with the dominant ground roll frequency. This is a subsurface artefact which prohibited the filtering of the ground roll with a frequency-dependent filter such as a wavenumber-frequency filter or a high-pass filter. The attenuation of high-frequency signal content in the polder is exemplified by Figure 22, which is a shot gather located on the fringe between the polder and non-polder and shows a wavefront propagating southward with a signal frequency peak at $\sim$ 40Hz and a wavefront propagating northward lacking this peak in frequency content. The test line terminates in the polder, however, the re-processed NAM-DEEP line from 1980s crosses the polder in its entirety and serves as a benchmark in order to verify if this frequency attenuating phenomenon is inherent to marine sediments in the polder (see Discussion).

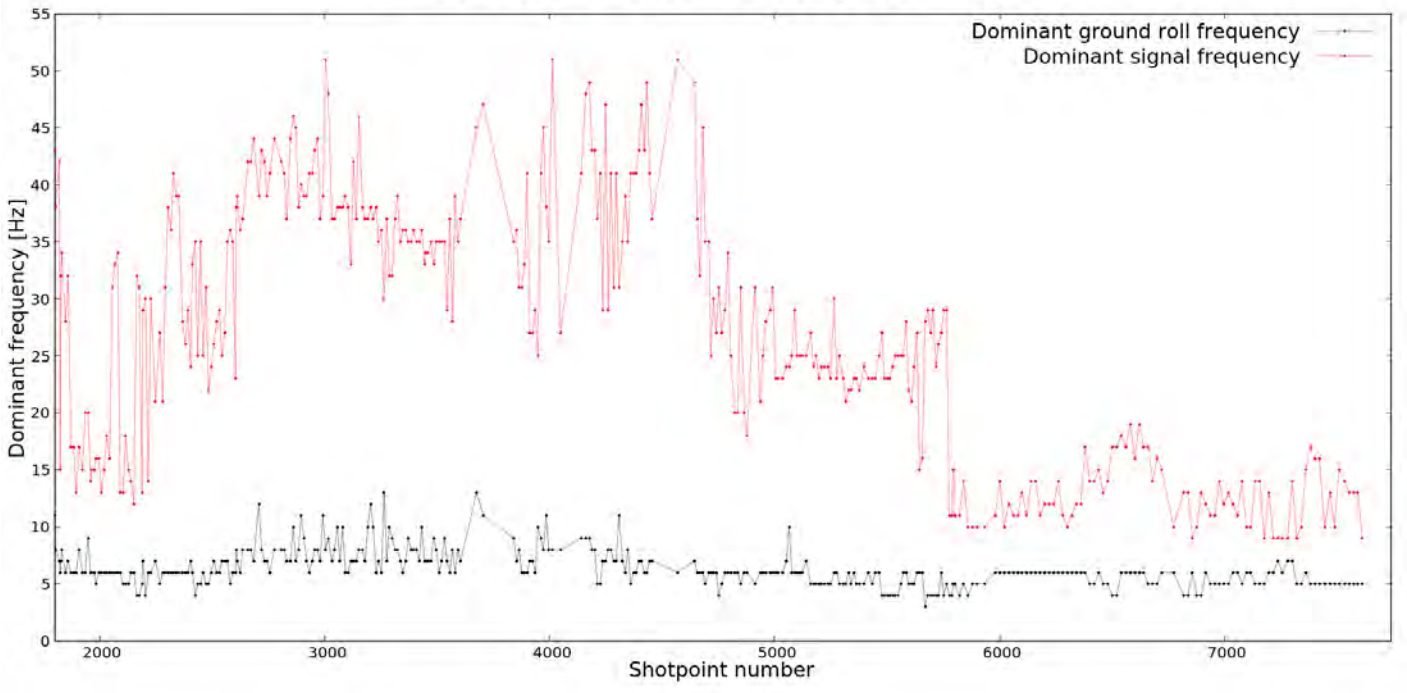

Figure 21: Hand-picked dominant frequency per shot gather of the ground roll (black) and of the signal (red).The figure excludes shots flagged as 'weak'. Left=SW, right=NE.

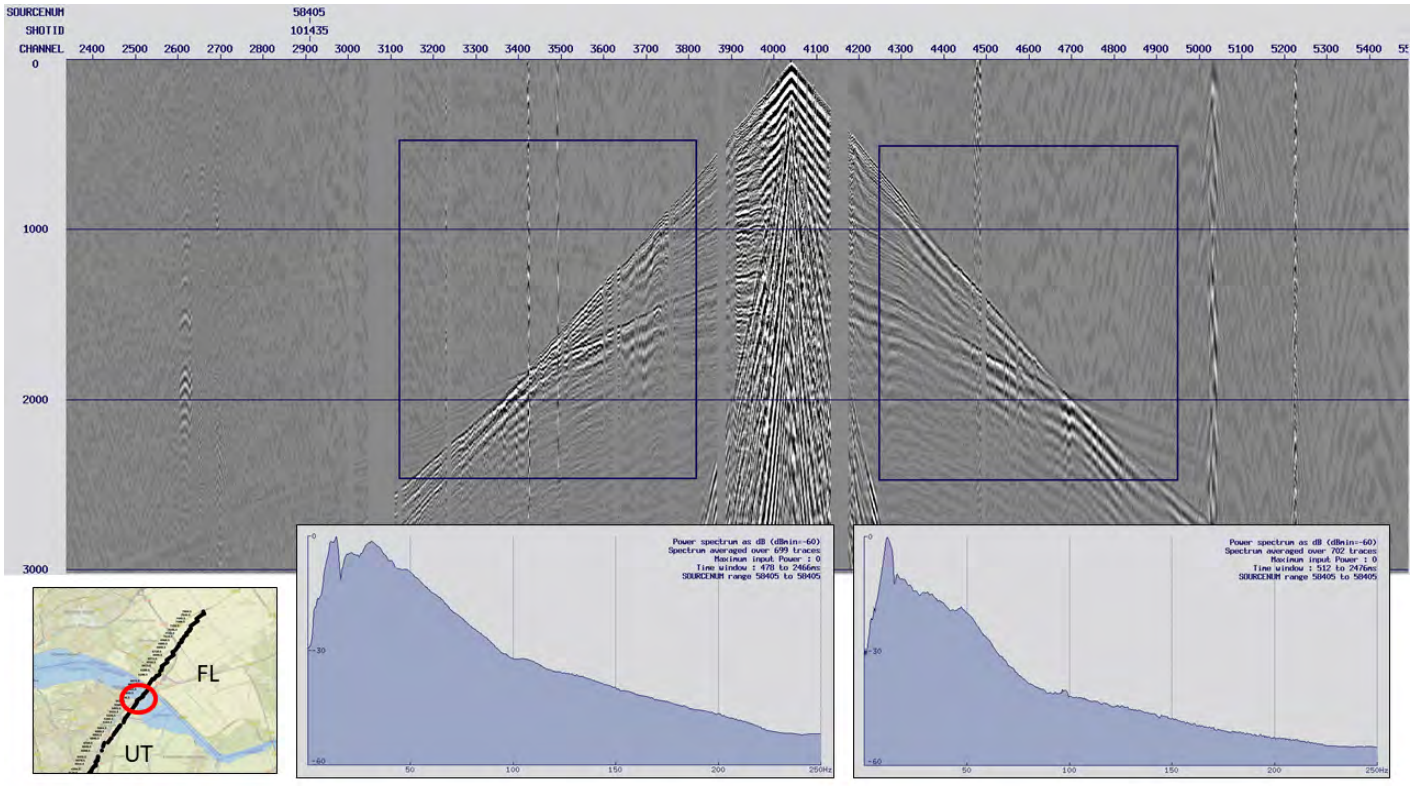

Figure 22: The discrepancy in frequency content exemplified by a shot on the fringe between the empoldered province of Flevoland (FL) and the 'mainland' province Utrecht (UT). Vertical axis of the shot gather states time in ms.

3.5 Uphole time & uphole velocity

Uphole times were measured during acquisition directly above the drill site, recording the time of arrival of the vertical wave. Figure 23 shows both the uphole times and the uphole velocities (normalized by shot depths). Shots acquired at shotpoint numbers 3188.5, 3212.5, 3220.5, 3232.5, 3236.5, 3964.5 were outliers due to suspected inaccurate recordings in uphole times and subsequently left out. Uphole times were measured with an accuracy of 1 ms. Generally, uphole velocities decrease with shallower shots due to the near surface being less consolidated and possibly less hydrated. Uphole velocities in non-polder areas range, on average, between 1000-1400 m/s. In the polder, uphole velocities decrease to approximately 600-800 m/s.

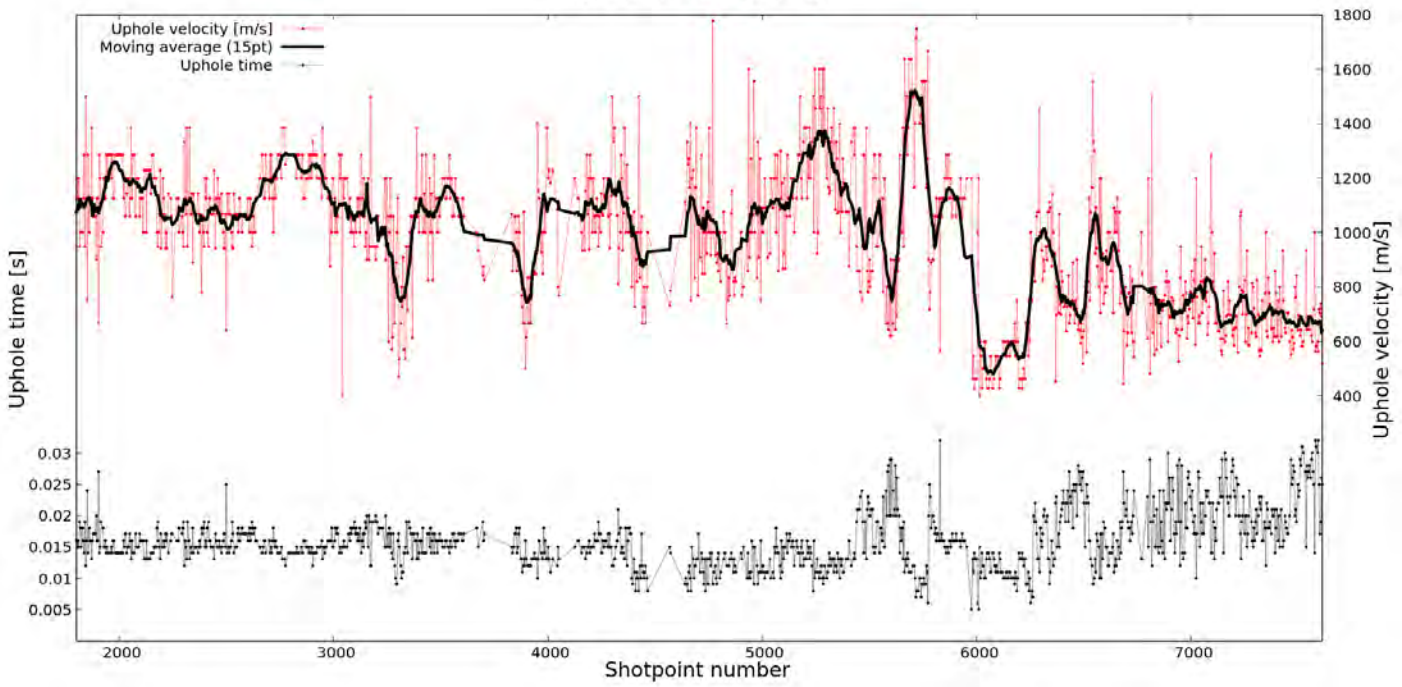

Figure 23: The uphole times (black) per shot gather and the uphole velocities (red) with a 15-point moving average. This figure excludes shots flagged as 'weak'. Left=SW, right=NE.

3.6 Ambient noise analysis in receiver domain

Instead of analyzing ambient noise per shot gather (all traces), looking at a single trace for all shots yields information regarding the relation between ambient noise and the localities of the receivers. The same time window has been used (19-20s) for the RMS amplitude measurements. Figure 24 shows the averaged RMS amplitudes per receiver along the test line. Figures 32 and 33 show noise amplitudes along the line in map-view.

Along the test line, sources of noise are: train tracks, highways (the test line passes the A27 national highway with a 130 km/h speed limit thrice), residential areas, windmills, industrial areas, tree lines, forest lines and solo trees. The test line passes underneath power lines once, however, this produces no substantial noise.

In this case, the ambient noise produced by highways could be seen in the data up to $\sim 180 - 200$m (Figure 26). Again, traces acquired after 5pm are significantly less noisy than traces acquired during the day (Figure 25). This is, presumably, due to decreased levels of traffic. The receivers placed around the train tracks are generally quiet but, as expected, a few traces show extraordinarily high amplitude ambient noise (up to 180, in contrast to normal noise amplitudes being 0.1-0.2). Out of 1355 shots, approximately 30 traces from this particular receiver show excessive noise amplitudes - which is presumably when a train passes by. These ~ 30 traces cause the receiver to be, on average, noisy. Noise from a passing train can be observed in the noise analysis up to ~ 40m (Figure 27).

The highest amplitude producing source of noise along the test line was windmills. The test line passed 2 windmills; one at ~ 50m and one passed right underneath (~ 10m). A signature of the windmills could be seen up to ~ 100m in the data (Figure 28). The second highest amplitudes are produced, surprisingly, by solo trees and tree lines. While the receivers placed within a forest are relatively quiet, it is receivers in the vicinity of solo trees, tree lines or forest lines that are noisy. Noise from trees does not propagate far; it can be seen until approximately 10m (Figure 29). Figures 30 and 31 show the chronological noise amplitudes of a single receiver underneath a windmill and a single receiver next to a noise-producing tree line versus wind speeds. Where the receiver next to a tree line shows a clear correlation wind speeds, the receiver underneath the windmill does not - suggesting influence from another external factor. Obtaining data of when this particular windmill was on or off was attempted, but to no avail.

It must be noted, however, that this noise analysis was performed on raw data. No anomalous trace editing was performed beforehand. This means that anomalous measurements might produce high average noise values for a receiver which is, in fact, relatively quiet (comparable to receivers next to the train tracks).

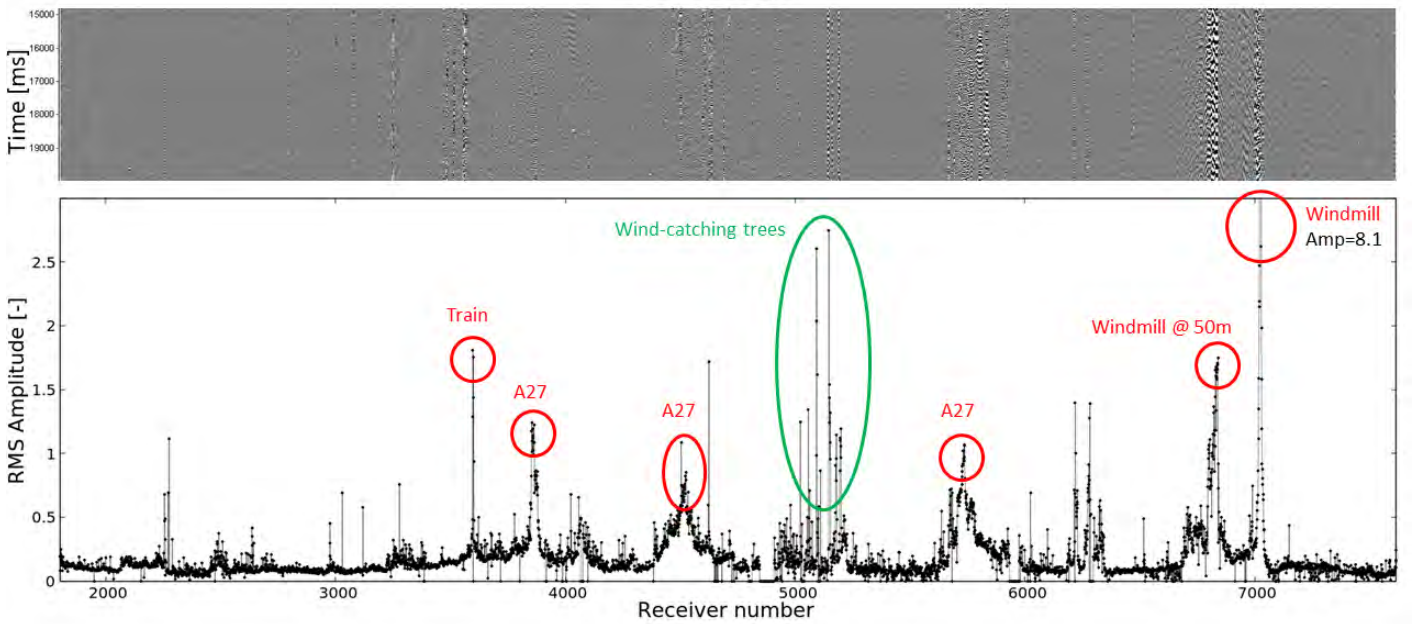

Figure 24: Sources of noise along the test line. The main culprits (train tracks, highways, tree lines and windmills) have been highlighted. Above, one shot record (SHOTID100693; 15-20s) without shot energy in order to visualize the noise. Please notice values exceeding the vertical axis. Left=SW, right=NE.

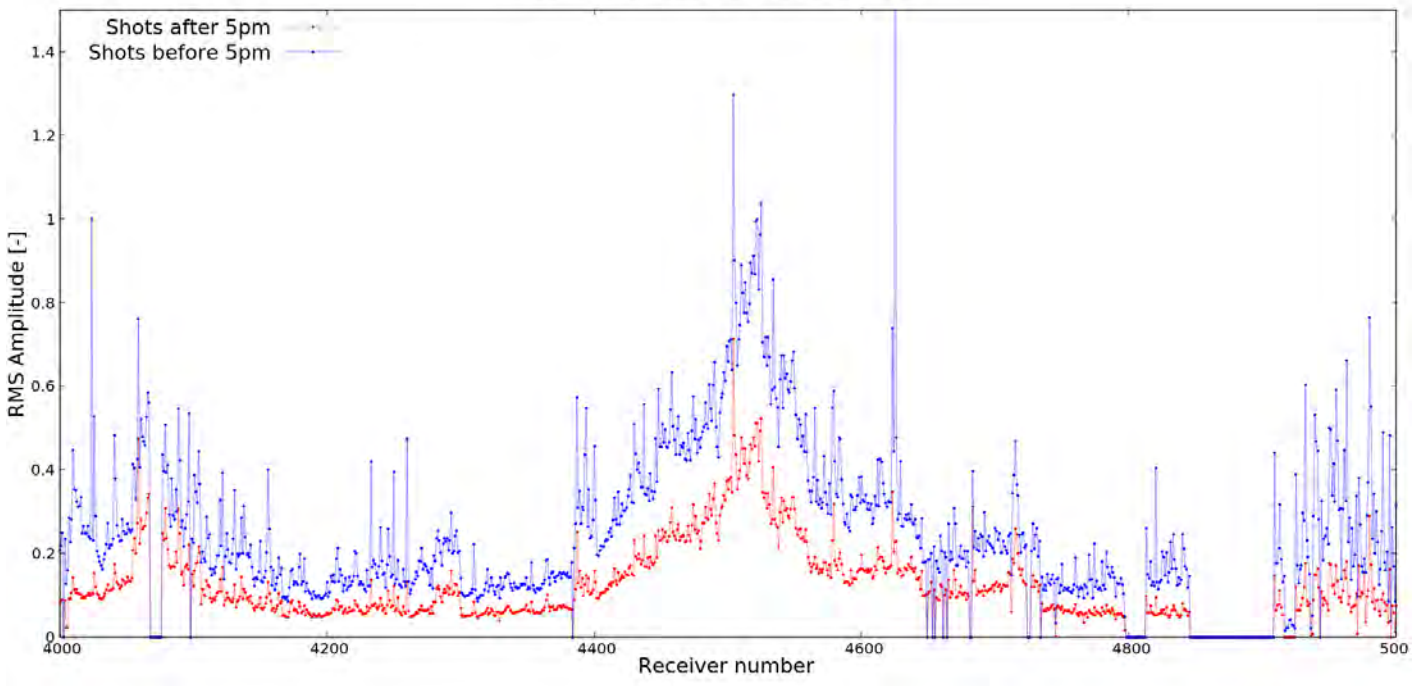

Figure 25: A zoom-in of the ambient noise measurement along the highway A27. The data is delineated into shots fired before (blue) and after (red) 5pm. Left=SW, right=NE.

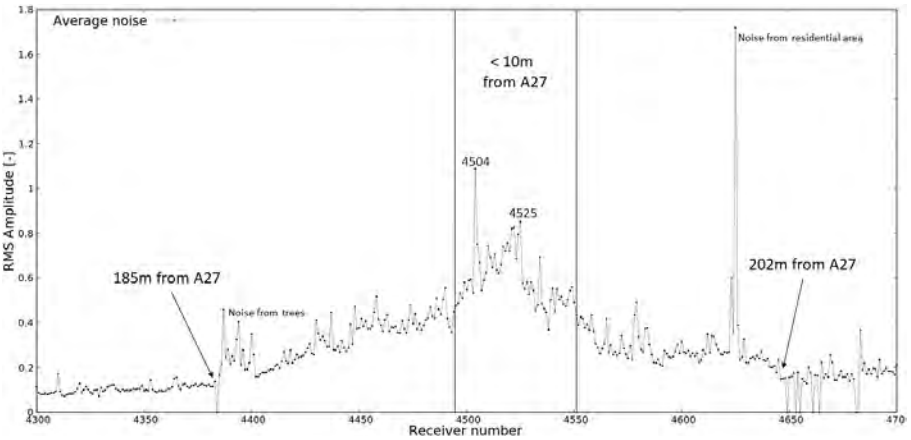

Figure 26: Highway A27 (130 km/hr) produced noise visible up to ∼185-202m.

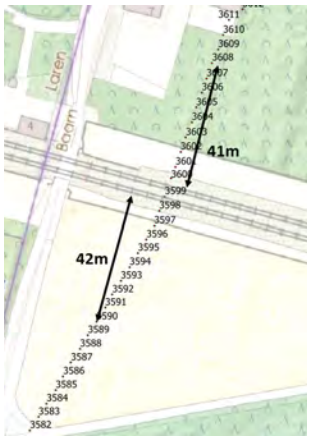

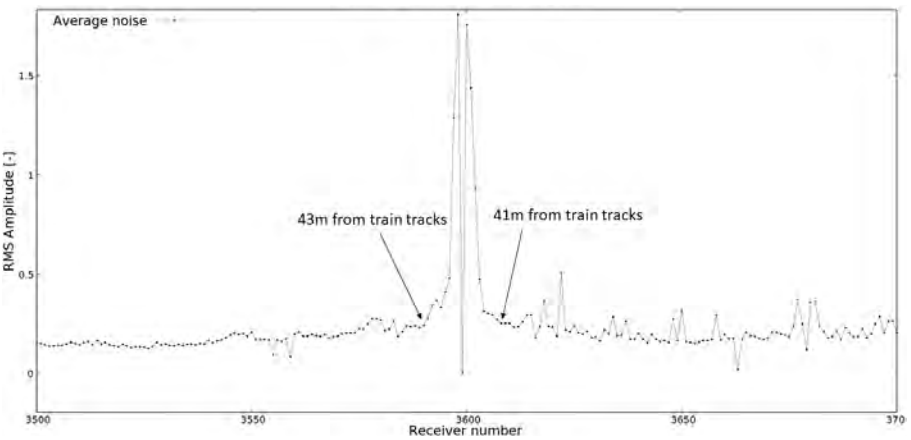

Figure 27: Train tracks produced noise visible up to ∼41-43m.

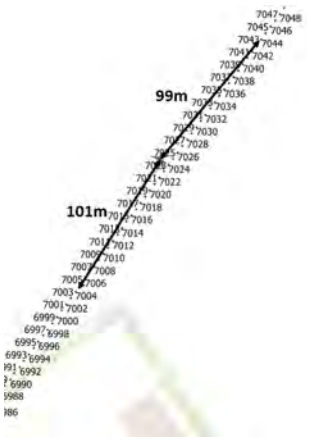

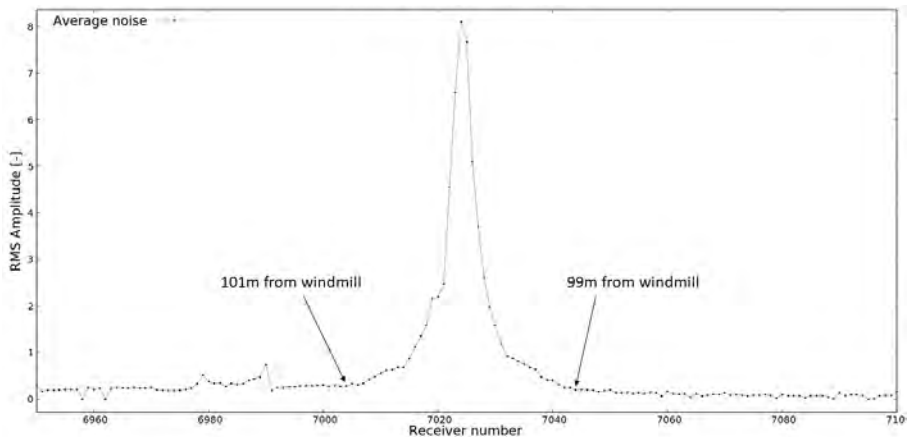

Figure 28: Windmills produced noise visible up to 99-101m.

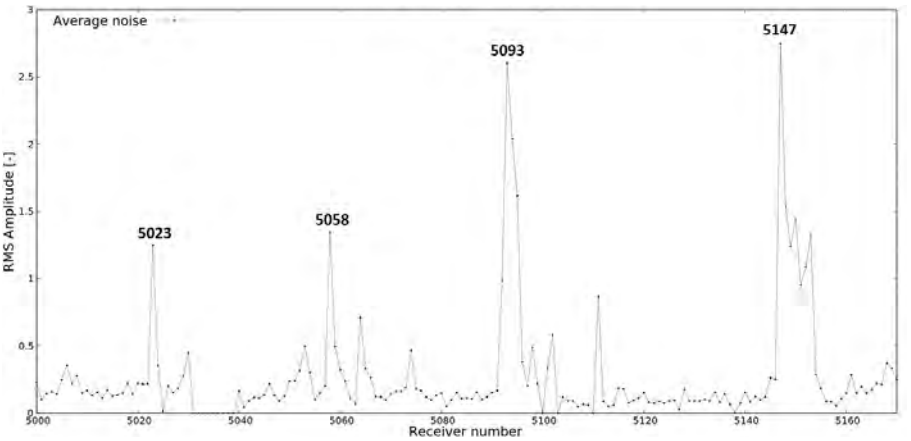

Figure 29: Tree lines produced noise visible up to ∼10m.

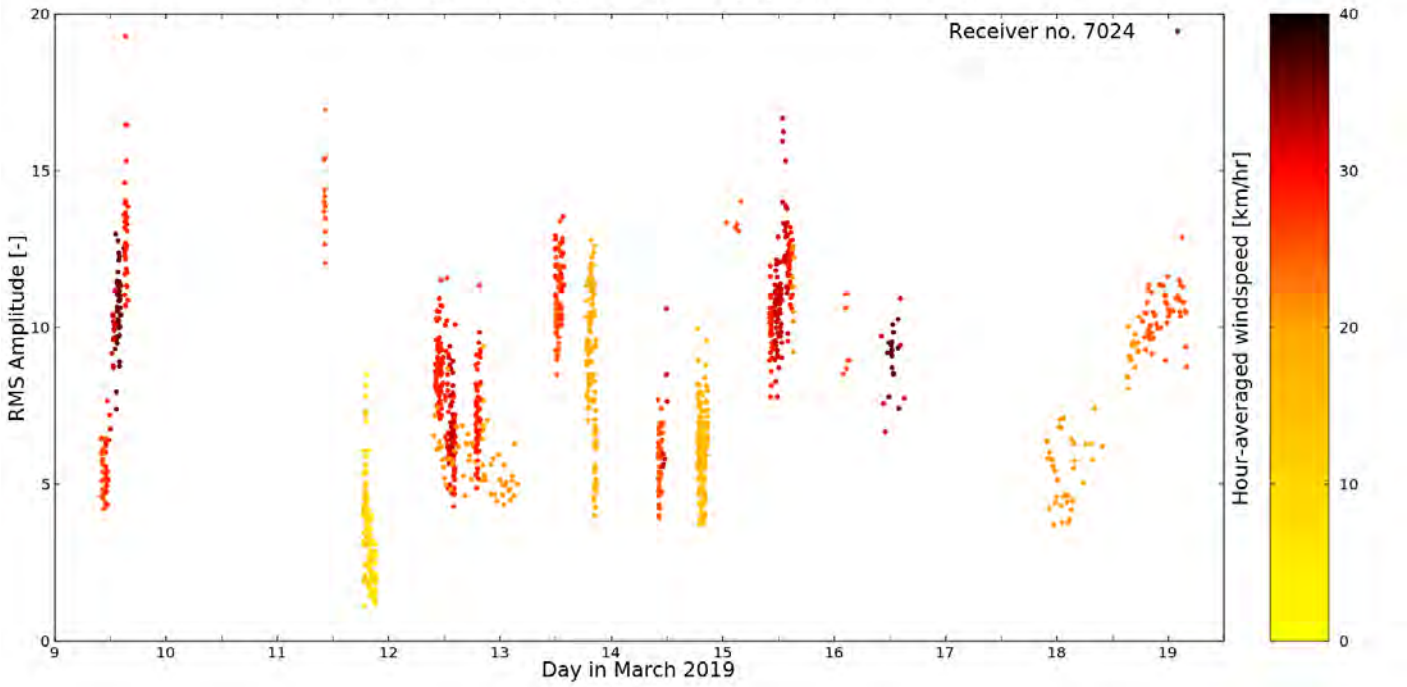

Figure 30: Chronologically, noise amplitudes from receiver no. 7024, which is right underneath a windmill. The colour coding is the hour-averaged wind speeds.

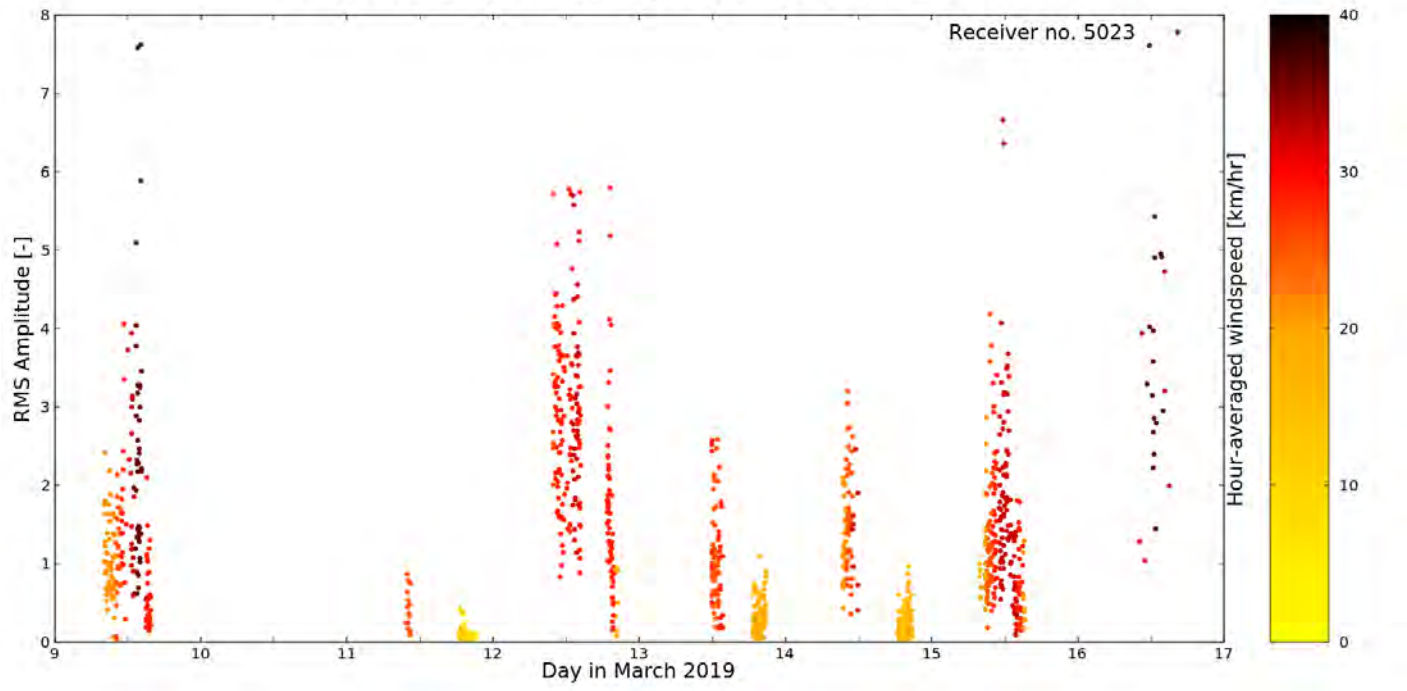

Figure 31: Chronologically, noise amplitudes from receiver no. 5023, which is next to a tree line on an empty pasture. The colour coding is the hour-averaged wind speeds.

Figure 32: Map-view (1:65000) of noise amplitudes in the receiver domain of the northern half of test line.

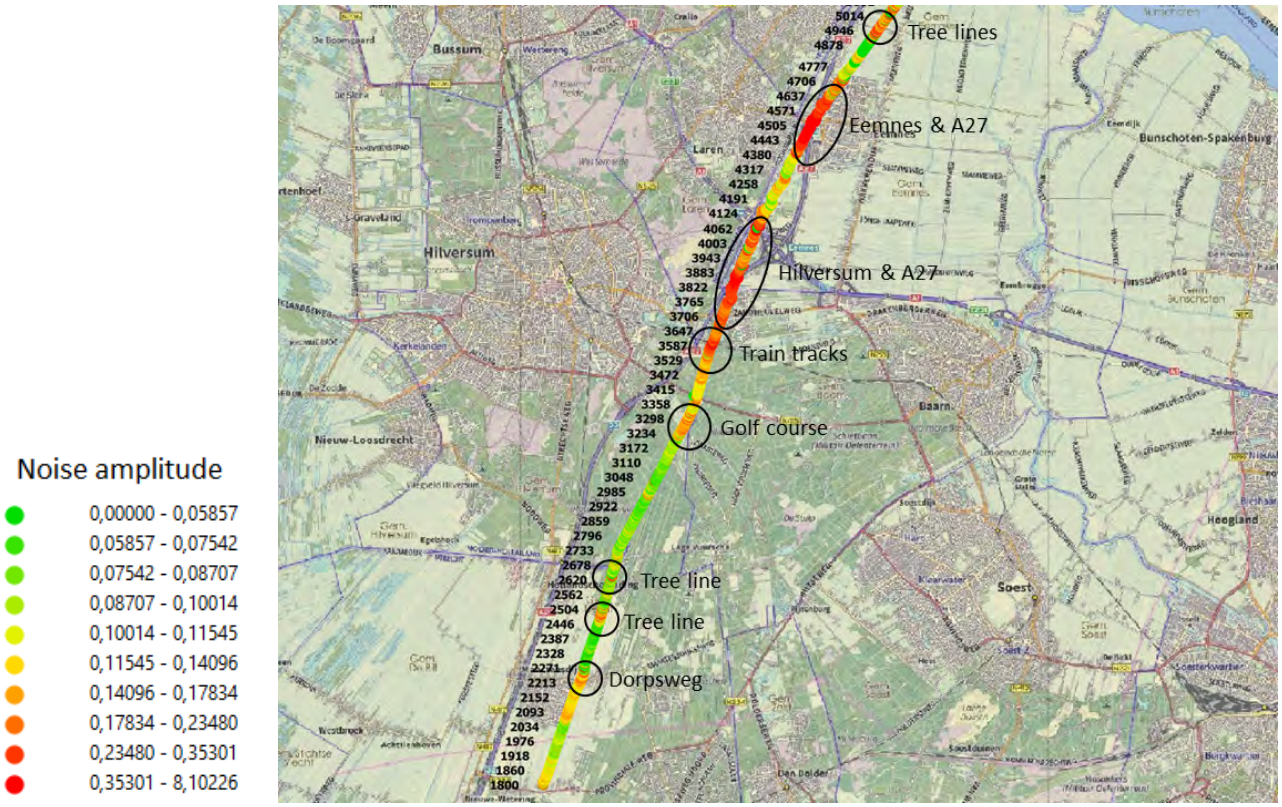

Figure 33: Map-view (1:65000) of noise amplitudes in the receiver domain of the southern half of test line.

3.7 Noise analysis on stacked data

To test the influence of noise on the quality of subsurface images, RMS amplitude analysis was performed on the final second (9-10s; does not contain seismic signal) of the stacked data (Figure 35). The stacked data in question has gone through the first steps in the processing sequence, including muting anomalous traces and filtering of ambient noise through a bandpass filter. In order to stack, seismic data is sorted to the CDP domain and therefore any noise that does not get muted or filtered in the processing should result in a smeared peak in RMS noise amplitude on the stack. Noise amplitude analysis was performed on 2 versions of stacked data (Figure 34). The increased amplitudes on both ends of the stack are a taper artefact.

The RMS amplitudes from the tenth second of the stacked data consistently yield a value around 0.2, which is the approximately the ambient noise amplitude value for quiet receivers along the test line. The stacks do not contain clear effect of ambient noise.

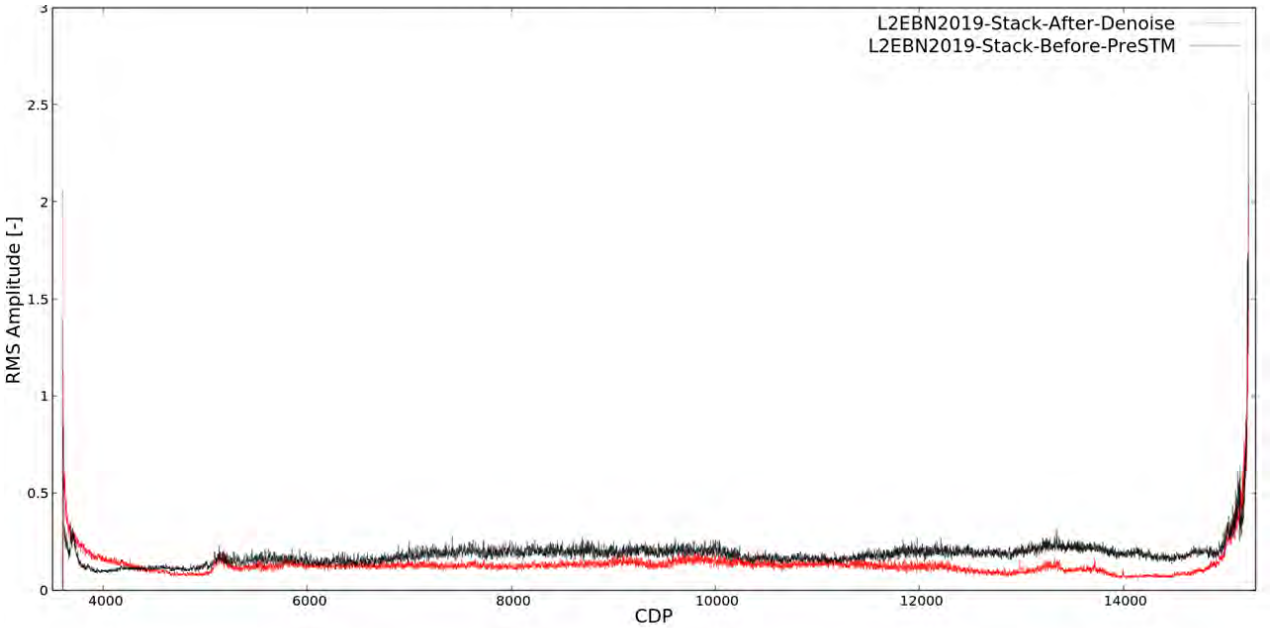

Figure 34: The RMS amplitudes of the last second of stacked data. Left=SW, right=NE.

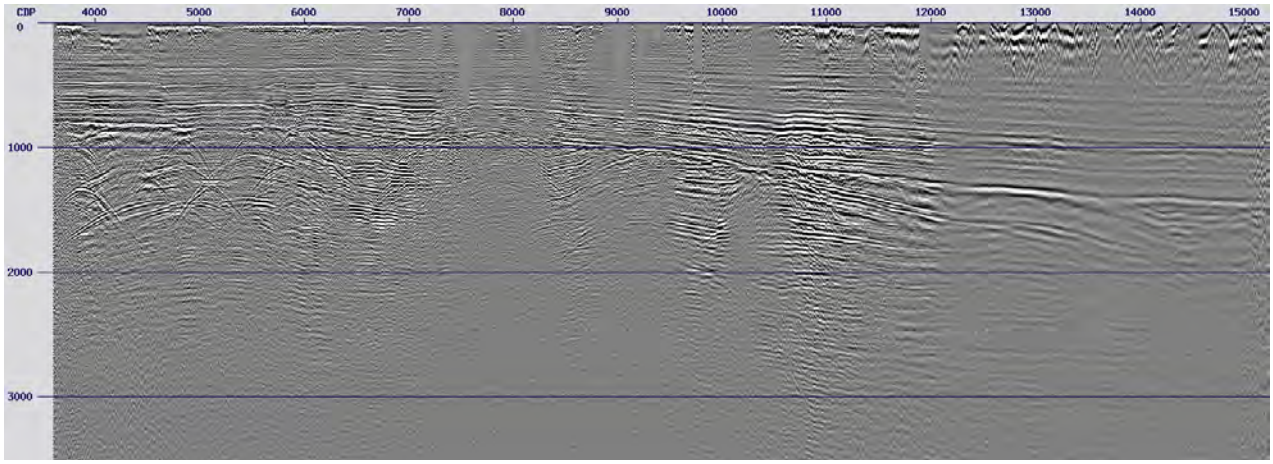

Figure 35: An example of a stack on which amplitude analysis was performed (L2EBN2019-Stack-After-Denoise; see Figure 34). Vertical axis states time in ms.

4 Discussion

4.1 Shot quality and geology

Geological models available at DINOloket (DGM, GeoTOP, REGIS II) are mere interpolations of well data. Thus, correlating shot quality to the geological models proved to be challenging, because:

- Geological models and their resolution are wholly dependent on the abundance, proximity and quality of well data (Figure 36).
- Geological models do not contain data regarding the topsoil and thus receiver coupling.

Figure 36: Map-view (1:165000) of the abundance and proximity of nearest wells utilized to construct subsurface models DGM and REGIS II

The overall trend in shot quality throughout the test line does not correlate to any (combination of) acquisition parameter(s) and must therefore be determined by the subsurface. Locally, shot quality is determined mostly by signal amplitude and thus charge size and shot depth. The signal amplitude and SNR unsurprisingly benefit from increased charge sizes and shot depths. Both parameters could potentially contribute to improved deep imaging and should, when operationally possible, be maximized. A favourable effect of increasing shot depth would be the expected decrease of ground roll amplitude.

Signal amplitudes between shotpoint numbers 2700-3500 yield the highest signal amplitudes along the test line. This is located near stowed glacial deposits yet have also been acquired in wooded areas where the subsurface might be more consolidated compared to cultivated pastures. However, it is difficult to distinguish between the two possibilities due to the questionable reliability of the geological subsurface models.

4.1.1 The polder problem

The lowest signal amplitudes, in combination with a lack of high-frequency content, have been acquired in the southern Flevopolder. Here, though usually shot with a 880-1000g at a depth of ≥10m, the signal amplitudes are consistently weak. Moreover, uphole velocities decrease to 600-800 m/s and the dominant signal frequency decrease to ∼10-15 Hz (as opposed to ∼25-45 Hz outside the polder). A local lack of high-frequency signal content will lead to a deterioration in vertical resolution in migrated images and stacks, as is visible in the test line PreSTM (Figure 37).

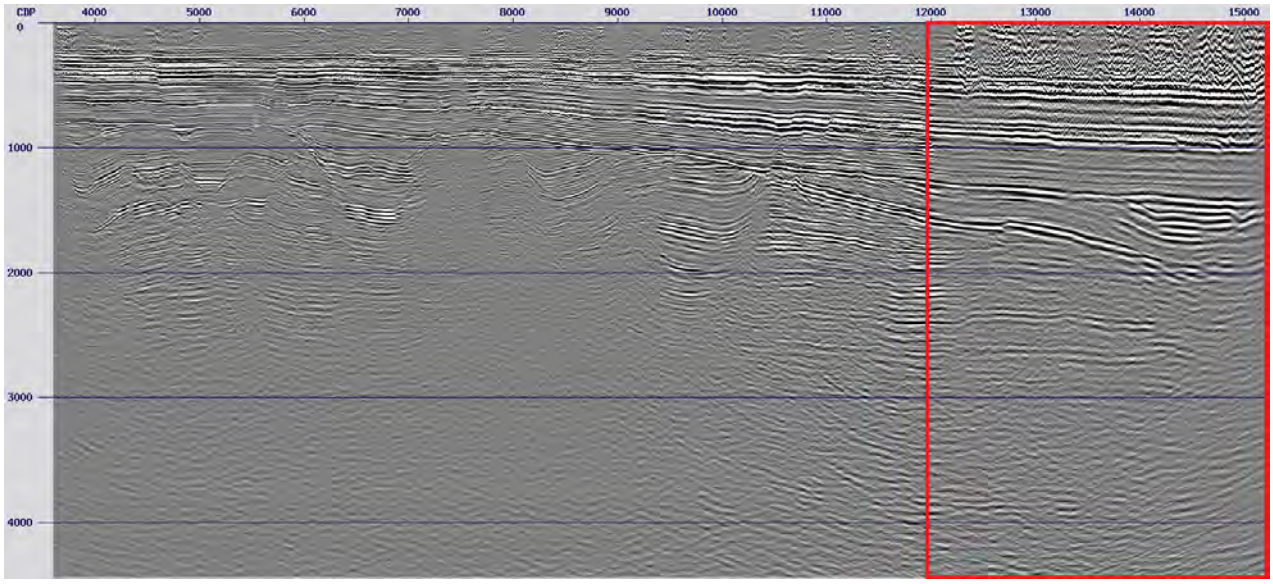

Figure 37: Test line final PreSTM, where a deterioration of vertical resolution is present in the northern part (right).

The test line terminates in the polder, however, the re-processed NAM-DEEP line from the 1980s crosses the polder in its entirety. The NAM-DEEP line reaffirms this phenomenon in the south(eastern) part of the polder, however, retrieves high-frequency signal content in the central and northern part of the polder (Figure 38). This change in frequency content is abrupt.

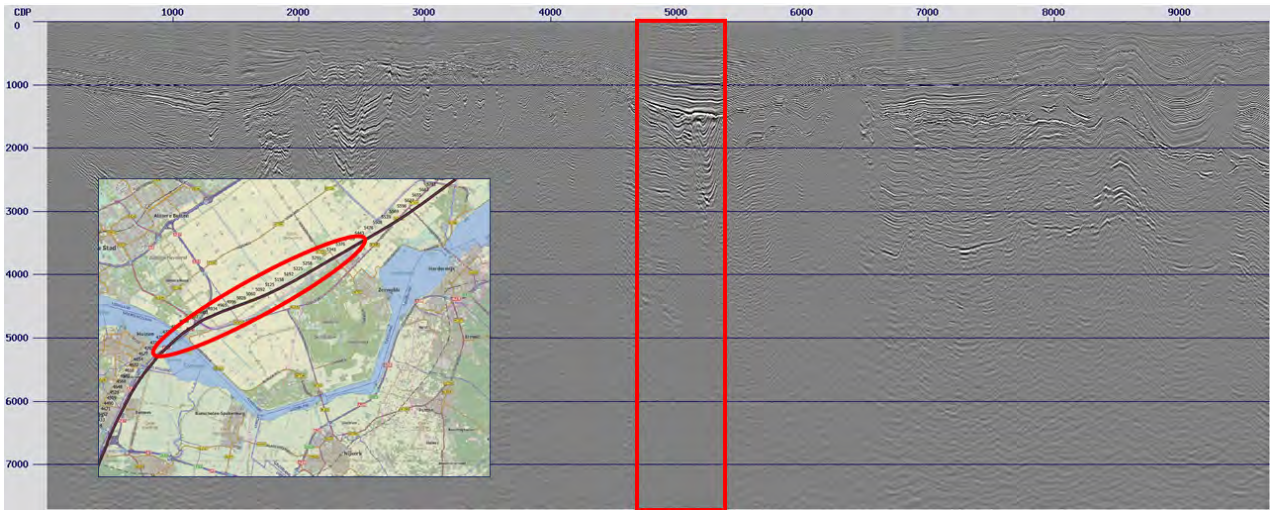

Figure 38: The NAM-DEEP final PreSTM with the empoldered area lacking high-frequency content marked in the red box (CDP's mapped on the left). Figure 39 shows a zoomed version in combination with a REGIS II geological cross-section.

Holocene marine clays are present throughout the empoldered region and are thereby an unlikely source of high-frequency attenuation. Based on REGIS II (Figure 39), low signal amplitudes in combination with a lack of high-frequency content in the southern Flevopolder has several potential attenuating culprits:

1. The Woudenberg peat formation (possible indication for a methane-saturated subsurface).
2. A thickened Eem-formation (possible undercompacted clays). Spatially, the area of thickening matches the area of high-frequency attenuation of the test line, the NAM-DEEP line and other vintage seismic data.
3. The Gieten-subformation (part of the Drenthe-formation; glacial deposits containing pebbles/boulders; possible sources of scattering).
4. A large contrast in seismic velocity underneath the slow Eem-formation. A velocity model for the test line was constructed through refraction tomography by the processing company Geofizyka Toruń, which was meant to serve as a starting point for a full waveform inversion algorithm. It shows a low velocity anomaly in the polder (reaffirmed by the slow uphole times), accompanied by a high velocity anomaly directly underneath it. This velocity contrast might be indicative of a large impedance contrast.
5. A combination of the aforementioned.

The fourth line with the SCAN-project will again traverse this area of high-frequency attention which offers a window for a follow-up study on the spatial dimensions of this attenuating body and potential correlation to the geology.

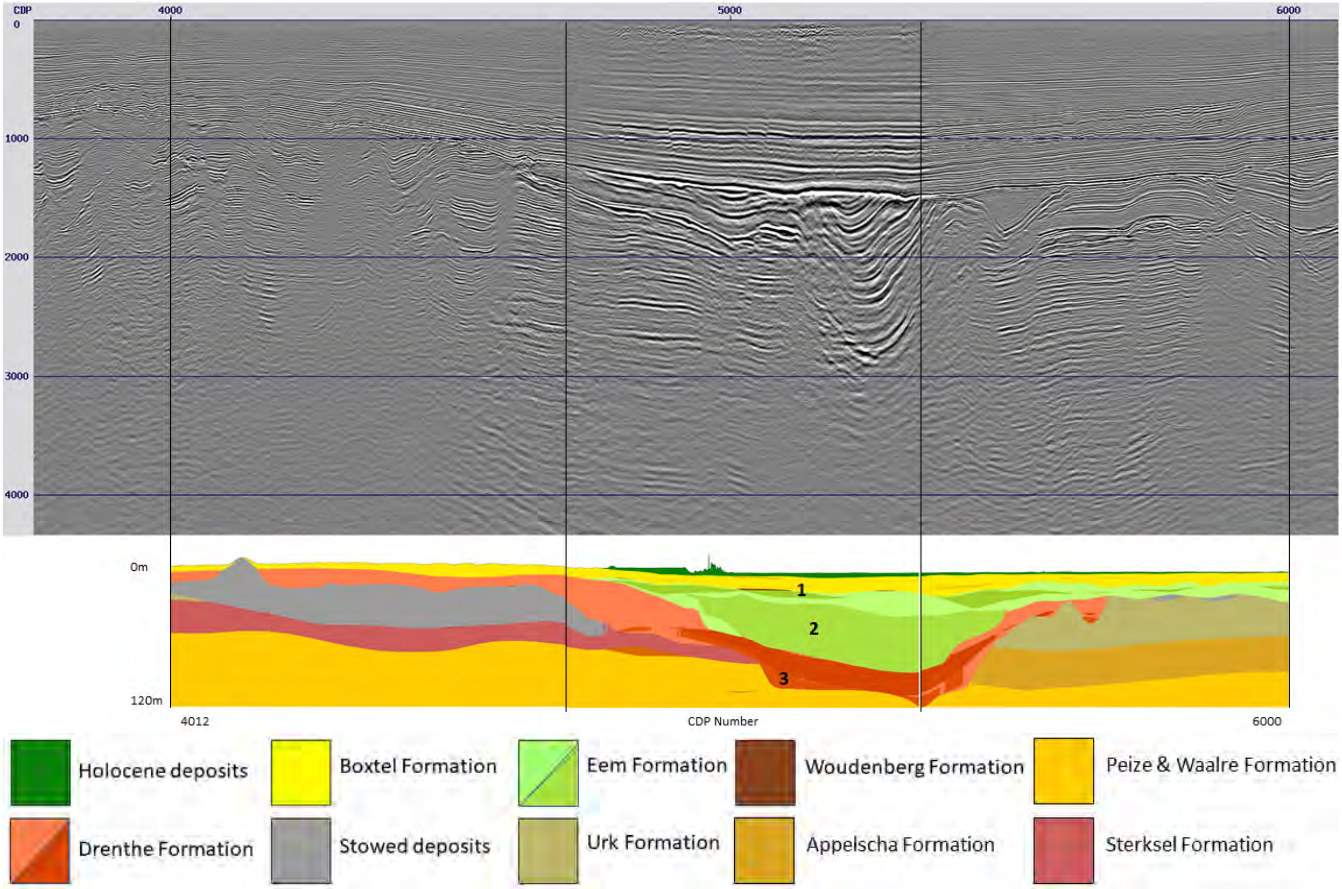

Figure 39: The area of the NAM-DEEP line that lacks high-frequency content and, below, a geological cross-section of model REGIS II. This figure is a zoomed-in version of Figure 38.

4.2 Noise mitigation

Sources of noise have been found to be traffic, windmills, train tracks, residential areas, industrial areas, tree lines, trees etc. Both analyses in the shot and receiver domain showed data acquired during the day and at high wind speeds to be the most noisy. Noise mitigation techniques could comprise of:

1. Keep distance from sources of noise:
    - ∼100m from windmills
    - ∼10m from trees
    - ∼200m from highways
    - ∼40m from train tracks
2. Shoot in the early morning or in the evening*.
3. Shoot with low wind speeds*.

**It must be noted that wind speeds and time of day are often mutually correlated; the afternoon is often the windiest time of day.*

Aforementioned, no anomalous trace editing was performed beforehand and therefore extreme outliers might influence the average noise amplitude per receiver. This analysis is based on noise amplitudes; no distinguishment has been made between coherent and non-coherent noise. Mitigating non-coherent noise is of lesser importance for it won't constructively stack in further processing.
Noise analysis of stacked data suggests the predominant noise is removed successfully during processing. Therefore, data quality seems mostly dependent on signal amplitudes rather than noise amplitudes. Hence, during acquisition, signal maximization should be prioritized over noise mitigation. This is the case, however, for a seismic survey performed with a shot spacing of 20m. The remainder of the SCAN-project is performed with a shot spacing of 60m and therefore already a decrease in SNR is expected. Here, noise might be more influential on the quality of stacks and migrated images.

5 Conclusion

The SCAN test line data quality has been investigated. The predominant factor is the subsurface, however, signal amplitudes can be enhanced by maximizing acquisition variables such as shot depth and charge size. High signal amplitudes show a potential correlation to stowed glacial deposits or wooded areas, yet differentiating between the two is hindered by the reliability of the geological models. The southeastern part of the Flevopolder is an area of low signal amplitudes and a lack of high-frequency content in both test line and vintage data, which has multiple potential sources of attenuation, the most likely being a thickened Eem-formation. Noise mitigation techniques could comprise of keep distance to known sources of noise or shooting at times of low wind speeds and traffic. Amplitude analysis on stacked proved noise mitigation might be of lesser importance than maximizing signal amplitudes, however, this does not take into account financial considerations (improvement of data quality through clever receiver placement does not come with extra acquisition costs).

References

Boxem, T., Veldkamp, J., and van Wees, J. (2016). Ultra-diepe geothermie: Overzicht, inzicht & to-do ondergrond. *TNO report*, page R10803.

Bruijnen, P. (2019). Estimating geothermal power of ultra-deep dinantian carbonates in the dutch subsurface. *SCAN report*.

Carlson, T. (2019). Petrophysical report of the dinantien carbonates in the dutch subsurface. *SCAN report*.

Gunnink, J., Maljers, D., Van Gessel, S., Menkovic, A., and Hummelman, H. (2013). Digital geological model (dgm): a 3d raster model of the subsurface of the netherlands. *Netherlands Journal of Geosciences*, 92(1):33–46.

Middelburg, M. and Drenth, D. (2019). A generic hazard inventory for drilling ultra-deep geothermal wells. *SCAN report*.